Dark Soliton Solutions of (2+1)-dimensional Gross-Pitaevskii Equation with Spatially–periodic External Potential

by

© **Zhe Huang**

A thesis submitted to the School of Graduate Studies in partial fulfillment of the requirements for the degree of Master of Science.

Department of Mathematics and Statistics

Memorial University

September 2017

St. John's, Newfoundland and Labrador, Canada

Abstract

In this thesis, we study the existence and stability of background solutions (BGSs) and dark soliton solutions (DSSs) of the Gross-Pitaevskii equation (GPE) with a spatially-periodic external potential in (2+1)-dimensional domain. First, we use dynamical systems theory to prove the existence of stationary solutions (BGS and DSS). Exponentially decaying coefficient of the dark soliton near the BGS is derived in terms of an eigenvalue problem. The stability/instability of the solutions is investigated in a weighted functional space. The critical wave numbers in the y direction are derived. We then consider two special cases: the case of large chemical potential and the case of slowly varying external potential. In both cases, we apply asymptotic analysis to obtain the approximate formulas for the stationary solutions. As such analytic results are obtained in both cases. All the results are supported by direct numerical computations of the stationary solutions as well as the computations of the corresponding eigenvalue problems.

Acknowledgements

I really appreciate to have the great opportunity to study at Memorial University and want to express my gratitudes to the people who have supported and helped me so much during my studies here.

I would first like to express my sincere gratitude to my supervisor Dr. Chunhua Ou for the immeasurable amount of support and guidance he has provided through the learning process of this master thesis. Dr. Ou's patience and brilliant advice helped me not only in the scientific arena, but also on a personal level.

I would also to acknowledge the faculty and staff at Department of Mathematics and statistics. Furthermore, I am especially grateful to my cosupervisor Professor Xiaoqiang Zhao for his excellent course and financial support throughout this study and Dr. Yuan Yuan for her great course and help.

I would also like to thank all the friends met here. Their daily smiles and intelligent suggestions have made my graduate life absolutely unforgettable and extremely enjoyable.

Finally, I must express very profound gratitude to my parents for providing me with continuous support and encouragement throughout my years of study.

Table of contents

Chapter 1

Introduction

Historically, the first experimental observation of the phenomenon about solitary waves could date back to 1834 by John Scott Russell. He observed a large protuberance of water without change in shape when it moved along the Edinburgh–Glasgow canal. He called the bulge of water the "great wave of translation" and reported it in his "Report on waves" in 1844 [43]. This remarkable scientific discovery inspired him to further explore the phenomenon. He conducted a series of experiments and revealed, empirically, that one of the most important relations between the speed v of a solitary wave and its maximum amplitude a above the free surface of liquid of finite depth h in the form: $v^2 = g(h + a)$, where g is the acceleration of gravity. Thus, these solitary waves are also called gravity waves (for more details please see [12] or [52]).

His experiments stimulated great interest in the subject of solitary waves. Many mathematicians and physicists have carried out a large amount of academic work. The first theoretical description of the solitary wave was owed to two Dutchmen Diederik J. Kortweg and Gustav de Vries in 1895. They analytically derived a nonlinear partial differential equation, the well-known KdV equation, which models the height of the surface of shallow water in the presence of a solitary wave. The KdV equation is a generic model for the study of weakly nonlinear long waves incorporating leading order nonlinearity and dispersion (for more details please refer to textbooks in nonlinear partial differential equations, e.g. [33] and [52]). Later, in 1965, Norman J. Zabusky and Martin D. Kruskal discovered that solitary waves sustain nonlinear interactions from the KdV equation. Moreover, they noticed that the waves emerging from this interaction maintain their original shape, amplitude and speed. This character resembles particle-like behavior. Motivated by this property, Zabusky and Kruskal started to call these solitary waves solitons [52, 54].

In order to provide a definition of a soliton, we first give the concept of a traveling wave. Based on [45], we have the definition as follows.

Definition 1.1. *Given an underlying equation, a traveling wave $\phi_w(\xi)$ is a solution which depends upon x and t through $\xi = x - vt$, where v is a fixed constant.*

Furthermore, solitary waves are the localized solutions in the class of traveling waves and the definition is given below.

Definition 1.2. *A solitary wave $\phi_{sw}(\xi)$ is a localized traveling wave; or, more precisely, a traveling wave whose transition from one constant asymptotic state as $\xi \to -\infty$ to (possibly) another as $\xi \to +\infty$ is essentially localized in ξ.*

Although the term soliton was originally applied to solitary waves coming from the KdV equation, there are now many other nonlinear equations possessing similar solutions without formal definitions. It is difficult to find a precise definition of a soliton, because the difference between solitary waves and solitons has become blurred in the physical literature. However, it is necessary for us to illustrate the definition. Thus, following Drazin and Johnson [13] and Scott et al. [45], we present the definition of a soliton as follows.

Definition 1.3. *A soliton $\phi_s(\xi)$ is a solitary wave solution with permanent form that asymptotically preserves its shape and velocity upon collision with other solitary waves.*

Solitons are found in many physical systems. With the development of techniques in computer science and physics, the interests in solitons grew rapidly. Especially, in recent years, the soliton structures in Bose-Einstein condensates (BECs) have attracted great attention. BECs were firstly predicted by Albert Einstein (1925) on the basis of a paper by Satyendra Nath Bose (1924). Due to the limitation of physical techniques, researchers could only develop theoretical work in the first decades. The experimental studies on the dilute atomic gases had no significant development untill the 1970s. With decades of development in experimental studies, the first realization of BECs finally happened in 1995. By combining different cooling techniques, the experimental teams of Cornell and Wieman at Boulder and of Ketterle at MIT finally succeeded in attaining the temperature and the densities required to observe BECs in vapors of ^{87}Rb and ^{23}Na [41]. After the first success, BECs were reported to be achieved in many other atomic species. From then on, a new era for solitons started.

To model the statics and dynamics of BECs, a quantum many-body approach is required [11, 14,19,41]. Specifically, an atomic gas, composed by N interacting bosons of mass m and confined by an external potential $V_{\text{ext}}(\mathbf{r})$, can be described by its many-body Hamiltonian, when the gas reaches the required dilute density and ultracold temperature. The many-body Hamiltonian is given in second quantization form by [41]

$$\begin{aligned} \hat{H} &= \int d\mathbf{r}\hat{\Psi}^{\dagger}(\mathbf{r},t)\left[-\frac{\hbar^2}{2m}\nabla^2 + V_{\text{ext}}(\mathbf{r})\right]\hat{\Psi}(\mathbf{r},t) \\ &+ \frac{1}{2}\int d\mathbf{r}d\mathbf{r}'\hat{\Psi}^{\dagger}(\mathbf{r},t)\hat{\Psi}^{\dagger}(\mathbf{r}',t)V(\mathbf{r}-\mathbf{r}')\hat{\Psi}(\mathbf{r}',t)\hat{\Psi}(\mathbf{r},t), \end{aligned}$$

where $\hat{\Psi}^{\dagger}(\mathbf{r},t)$ and $\hat{\Psi}(\mathbf{r},t)$ are the boson annihilation and creation field operators respectively and $V(\mathbf{r}-\mathbf{r}')$ is the two-body interatomic potential. Apparently, it is problematic to treat the underlying many-body problem analytically as N increases; thus a mean-field approach is introduced. Adopting the well-established mean-field approximation, we have

$$\hat{\Psi}(\mathbf{r},t) = \langle\hat{\Psi}(\mathbf{r},t)\rangle + \hat{\Psi}'(\mathbf{r},t) = \Psi(\mathbf{r},t) + \hat{\Psi}'(\mathbf{r},t).$$

Here, the complex function Ψ is a classical field satisfying $\Psi(\mathbf{r},t) = \langle\hat{\Psi}(\mathbf{r},t)\rangle$ (which is the expectation value of the field operator) and having the meaning of an order parameter and commonly known as the *macroscopic wave function of the condensate*. $\hat{\Psi}'(\mathbf{r},t)$ describes the non-condensed part, which accounts for quantum and thermal fluctuation. When the temperature reaches below T_c, it is reasonable to neglect the term $\hat{\Psi}'(\mathbf{r},t)$ (for more explanation please refer to [19]). To simplify the interatomic interaction potential, $V(\mathbf{r}-\mathbf{r}')$, we consider the case of this dilute ultracold gas with binary collisions at low energy, characterized by the s-wave scattering length a. Under this limit, the interatomic potential can be replaced by $V(\mathbf{r}-\mathbf{r}') = g\delta(\mathbf{r}'-\mathbf{r})$, which is an effective delta-function interaction potential, where the coupling constant g is given by $g = \frac{4\pi\hbar^2 a}{m}$. Under these assumptions, from the Heisenberg representation $i\hbar(\partial\hat{\Psi}/\partial t) = [\hat{\Psi}, \hat{H}]$ for the field operator $\hat{\Psi}(\mathbf{r},t)$ and replacing the field operator $\hat{\Psi}(\mathbf{r},t)$ by the classical field $\Psi(\mathbf{r},t)$, i.e. neglecting the term $\hat{\Psi}'(\mathbf{r}',t)$, we could obtain a nontrivial zeroth-order theory for the BECs wave function. The above consideration leads to the famous Gross-Pitaevskii equation (GPE), which can be expressed as

$$i\hbar\partial_t\Psi(\mathbf{r},t) = \left[-\frac{\hbar^2}{2m}\nabla^2 + V_{\text{ext}}(\mathbf{r}) + g|\Psi(\mathbf{r},t)|^2\right]\Psi(\mathbf{r},t). \tag{1.1}$$

In above equation, $\Psi(\mathbf{r},t)$ is normalized to the number of atoms N, that is,

$$N = \int |\Psi(\mathbf{r},t)|^2 d\mathbf{r}. \tag{1.2}$$

The GPE (1.1) was derived independently by Eugene P. Gross [15] and Lev P. Pitaevskii [42] in 1960s. It is the main theoretical tool to investigate nonuniform dilute Bose gases in the frame of the mean-field theory. The mean-field approximation is strictly valid under three conditions: the first one is that the total number of atoms should be large enough; the second one is that the diluteness condition is satisfied and the temperature should be in the limit of zero; the last one is that the distances between atoms are much larger than the scattering length [41]. Moreover, Equation (1.1) can be treated as a variant of the well-known nonlinear Schrödinger equation (NLSE) incorporating an external potential [10].

In fact, the solutions of the GPE contain a large range of physical phenomena, including interference, quantized vortices, collective oscillations, expansion, solitons and so on [41]. Among those phenomena, the soliton solutions are regarded as one of the most important ones, because both matter-wave solitons and optical solitons can be viewed as fundamental nonlinear exitations of the GPE. Furthermore, solitons are viewed as fundamental nonlinear excitations of BECs in 1D; vortices are the excitations in 2D and etc. In this thesis, we only care about soliton solutions; thus, in the following, all the background information is about solitons. Basically, soliton solutions can be divided into two basic classes based on the sign of the nonlinearity which is introduced by interatomic interactions. The sign of g, which sets the directon of force between atoms, may take either positive or negative signs; that is because of the fact that the s-wave scattering length a may take $a > 0$ (e.g., for rubidium BECs) or $a < 0$ (e.g., for lithium BECs).

These two cases separately correspond to repulsive and attractive force between atoms, or to defocusing and focusing Kerr-type nonlinearites in the language of nonlinear optics [19]; thus soliton solutions are classified to the dark and bright soliton solutions (with DSS for dark soliton solution and BSS for bright soliton solution in the following context).

We also notice that Equation (1.1) can be written in a canonical form

$$i\hbar\frac{\partial}{\partial t}\Psi = \frac{\delta E}{\delta \Psi^*},$$

where $*$ denotes complex conjugate and the dynamically conserved energy functional E is given by

$$E = \int dr \left[\frac{\hbar^2}{2m}|\nabla\Psi|^2 + V_{\text{ext}}|\Psi|^2 + \frac{1}{2}g|\Psi|^4\right]. \tag{1.3}$$

In the above equation, the three terms from right-hand side denote the kinetic energy, the potential energy and the interaction energy, respectively. In [26], there is a rigorous mathematical proof that the GP energy functional describes the ground state of a dilute Bose gas of particles interacting with repulsive forces.

Now, we take the GPE (1.1) in a simple form in the case of stationary solutions. Here the BECs evolve in time according to the law as:

$$\Psi(\mathbf{r}, t) = \Psi_0(\mathbf{r})e^{-i\mu t/\hbar}.$$

In the law, the time dependence is fixed by the chemical potential

$$\mu = \frac{\partial E}{\partial N}.$$

After substituting the above two equations into (1.1), the GPE reduces to

$$\left[-\frac{\hbar^2}{2m}\nabla^2 + V_{\text{ext}}(\mathbf{r}) - \mu + g|\Psi_0(\mathbf{r})|^2\right]\Psi_0(\mathbf{r}) = 0. \tag{1.4}$$

Here we have assumed that the external potential only depends on the space variable. In Equation (1.4), μ denotes the chemical potential and Ψ_0 is a real function with the normalization condition $\int |\Psi_0(\mathbf{r})|d\mathbf{r} = N$.

In the Thomas-Fermi (TF) approximation, the ground state configuration takes a particularly simple form. In fact, the quantum pressure associated with kinetic energy term becomes significant near the boundaries and can be neglected elsewhere. Thus, it is safe to neglect the laplacian term in the Equation (1.4), which directly leads to the following density profile

$$n(\mathbf{r}) \equiv |\Psi_0|^2(\mathbf{r}) = g^{-1}[\mu - V_{\text{ext}}(\mathbf{r})]$$

in the region where $\mu > V_{\text{ext}}(\mathbf{r})$ and $n = 0$ elsewhere.

The main purpose of this thesis is to investigate further the dark soliton solutions of Equation

(1.4). Thus, we first briefly review some of the current work.

As we know, the NLSE and the GPE both allow the existence of the DSS. Now, we start with the NLSE. The pioneer work of the DSS in the NLSE was due to the paper by T. Tsuzuki [50] (in this paper, the author called the NLSE as PG equation), where exact soliton solutions were obtained and their connection with Bogoliubov's phonons [5] was revealed. Another important paper for the NLSE was from V. E. Zakharov and A. B. Shabat [56], they solved the NLSE exactly by the method of the inverse scattering transform. Through this method (also can be seen in [1, 55]), one can solve the NLSE and obtain multisoliton solutions. Moreover, in 1D case, stationary solutions have been found under box and periodic boundary conditions, see the repulsive case in [8] and the attractive case in [9] respectively. The perturbation theory for DSS was first introduced in [51] and later in [24] with a different mathematical statement. The variational approaches with some modifications were also used to seek DSS by investigating the width and the height of the solitons [3, 21]. As for the stability/instability studies, researchers were able to give the stability criterion in 1D case [4, 34] and investigated the dynamics of solitons [6, 22, 27, 40].

Adding an external potential term to the NLSE gives the GPE. It is clear that different types of external potentials result in different types of motion for the solitons. Considering physical background, there are three typical potentials which are commonly used to confine BECs. One is the parabolic potential (also known as the harmonic trap). When it appears, a systematic asymptotic multi-scale expansion method was used to get the approximation in 1D case [39]; the dynamics of bright and dark solitary waves were analytically studied in [47]. Another one is the potential barrier which is thought to be a bounded and exponential decaying function. When it appears, the analytical results of existence and stability of dark solitons in 1D case were given in [38]; the transverse instability of dark solitons and nucleation of vortices in 2D case have been investigated in [31]. The last one is referred as an optical lattice (OL) which is assumed to be a bounded and spatially periodic function. The OL potential is applied to investigate many important physical phenomena in quantum physics. When it appears, the existence of stationary DSSs for a cubic nonlinear term has been proved in [53], applying the upper and lower solution method and interpreting the DSS as a heteroclinic orbit. With the help of the dynamics of planar homeomorphisms, even when a quintic term occurs, the existence of stationary DSSs has also been proved in [48]. By improving classical variational approximation theory, the analytical expressions of both the BSS and the DSS were found, see [29] for the BSS and [30] for the DSS respectively. For a special case, even the exact solution could be found in the presence of external source in [17]. The stability and instability of DSSs confined in a harmonic trap and an OL have been studied in [18, 36]. Further, the dynamics of matter wave solitons has been investigated in [2, 7, 23, 28] and the existence, bifurcations and stability of gap solitons have been developed in [37]. It is seen that the motion of DSSs could be controlled by an OL in [46].

In this present work, we consider a (2+1)-dimensional GPE with a spatially-periodic external

potential. The (2+1)-dimensional GPE in a normalized form is (see [31])

$$i\frac{\partial u}{\partial t} = -\frac{1}{2}\left(\frac{\partial^2 u}{\partial x^2} + \frac{\partial^2 u}{\partial y^2}\right) + g|u|^2 u + V(x,y)u,\ x \in \mathbb{R},\ y \in (-\pi, \pi) \tag{1.5}$$

where $u(x, y, t)$ represents the macroscopic wave function of the condensate. The parameter g stands for the direction of interactive force between atoms, and $g = -1$ represents the attractive force corresponding to the BSS, while $g = +1$ represents the repulsive force corresponding to the DSS. In the present paper, we are interested in the DSS. Thus in the following context we fix $g = +1$. The external potential $V(x, y)$ is assumed to be

$$V(x, y) = A(x), \tag{1.6}$$

where $A(x)$ is a real periodic function with prime period L. For example, we can take $A(x) = V_0 \cos^2(kx)$, where V_0 is the strength of the potential, and k is the frequency of the potential. Thus, $A(x)$ is an even periodic function in x with the period $L = \frac{\pi}{k}$. The potential $A(x)$ is often referred as an OL and can be generated by the interference pattern of counter-propagating laser beams [46].

In the absence of external potential, i.e. $V(x, y) = 0$, Equation (1.5) admits an exact analytical solution for solitons. Assuming that its nodal plane is constrained along the x direction, then the DSS has following form [31, 46]

$$u(x, y, t) = u_0\{\mathcal{B}\tanh[u_0\mathcal{B}(x - vt)] + i\mathcal{A}]\}\exp\{-i\mu_0 t\}, \tag{1.7}$$

where u_0 denotes the amplitude of the uniform background of the dark soliton, and $\mu_0 = u_0^2$ is the dimensionless chemical potential. Here, $\mathcal{A} = \sin(\varphi)$ and $\mathcal{B} = \cos(\varphi)$, and φ is the phase shift across the DSS with $|\varphi| < \frac{\pi}{2}$. Moreover, $u_0\mathcal{B}$ and $u_0\mathcal{A}$ denote the amplitude (depth) and velocity of the DSS, respectively. The dark soliton is called black (grey) dark soliton when $\varphi = 0$ ($\varphi \neq 0$).

When the external potential is switched on, it is difficult to find analytical formulas of dark solitons for the GPE. In the present paper, we seek its solution with the following form

$$u(x, y, t) = v(x, y, t)e^{-i\mu t}, \tag{1.8}$$

where μ is a real constant and referred as the chemical potential. By substituting (1.8) into (1.5), we get the equation for function $v(x, y, t)$ as

$$iv_t = -\frac{1}{2}(v_{xx} + v_{yy}) + (A(x) - \mu)v + |v|^2 v. \tag{1.9}$$

Here, we impose periodic boundary condition at the boundary $y = \pm\pi$. To summarize, we

consider the solution $v(x, y, t)$ to satisfy

$$\begin{cases} iv_t = -\frac{1}{2}(v_{xx} + v_{yy}) + (A(x) - \mu)v + |v|^2 v, \ x \in \mathbb{R}, \ y \in (-\pi, \pi), \ t > 0, \\ v(x, -\pi, t) = v(x, \pi, t), \ v_y(x, -\pi, t) = v_y(x, \pi, t). \end{cases} \tag{1.10}$$

As shown in the above equation, the external potential is only a function of x. Thus we look for stationary DSS $v(x, y, t) = v(x)$ that is homogeneous in y direction and satisfies the following equation

$$\frac{1}{2}v_{xx} + (\mu - A(x))v - v^3 = 0, \tag{1.11}$$

subjects to boundary conditions

$$v(x) - U_+ \to 0 \ \text{ as } \ x \to +\infty, \quad \text{and} \quad v(x) - U_- \to 0 \ \text{ as } \ x \to -\infty. \tag{1.12}$$

Here, $U_\pm$ are real, bounded and L-periodic solutions of Equation (1.11) and also known as the background solutions (BGSs).

Through numeric computation, we illustrate the concepts of the BGS and the DSS in Figure 1.1. For the numeric scheme used here, please refer to Section 2.3. As shown in Figure 1.1, the

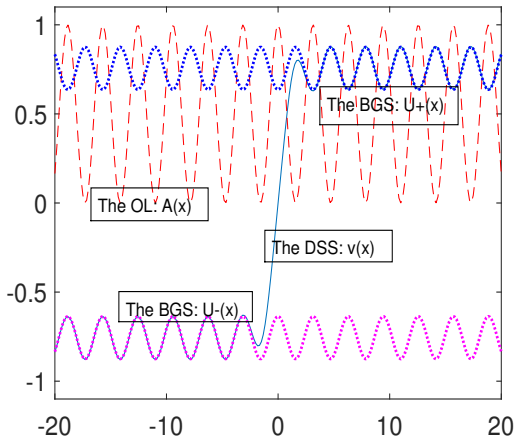

Figure 1.1: (Color online) The the BGS and DSS of (1.11). The figure corresponds to the parameter set: $A(x) = \cos^2(x)$, $\mu = 1.05$ and $x \in [-20, 20]$.

dashed line is the external potential $A(x)$, and the upper dotted line is the positive BGS $U_+(x)$, and the lower dotted line is the negative BGS $U_-(x)$. The solid thin line connecting $U_+(x)$ and $U_-(x)$ is the DSS $v(x)$ which is a heteroclinic connection.

The thesis is organized as follows. In Chapter 2, we use dynamical systems theory to prove the existence of the BGS and investigate the asymptotic behavior of the DSS as $x \to \pm\infty$. Then by means of linear stability analysis, we show the critical wave numbers of stability/instability of the BGS and the DSS. In Chapter 3, we consider the case where the chemical potential μ is large. In this case, $1/\mu \ll 1$ is a small parameter, so we could apply asymptotic analysis

to find the asymptotic formulas for the BGS and the DSS respectively. We also study the linear stability/instability of those stationary solutions and predict the critical wave numbers. In Chapter 4, we consider the slowly varying external potential case, that is, the external potential is replaced by "$A(\epsilon x)$" with $\epsilon \ll 1$. We derive asymptotic expressions of the BGS and the DSS. Then, we investigate the linear stability/instability of the stationary solutions and find out the corresponding critical wave numbers. Finally, in Chapter 5, we present the summary and future work of this thesis.

Chapter 2

Dynamics of (1.10)

In this chapter, we consider the existence of stationary solutions and their linear stability/instability for (1.10). We start from the following equation

$$iv_t = -\frac{1}{2}(v_{xx} + v_{yy}) + (A(x) - \mu)v + |v|^2 v,\ x \in \mathbb{R},\ y \in (-\pi, \pi),\ t \geq 0, \tag{2.1}$$

As discussed in the introduction, the stationary solutions contain the BGS and the DSS and satisfy the following equation

$$\frac{1}{2}v'' + (\mu - A(x))v - v^3 = 0, \tag{2.2}$$

where " $'$ " denotes the derivative with respect to x. Based on the above equations, we study the existence and linear stability of the stationary solutions in the following sections.

2.1 The stationary solutions

To find the stationary solutions, we need consider the BGS and the DSS separately, because they satisfy different boundary conditions at infinity.

We start with proving the existence and uniqueness of the BGS. To this end, we give a condition on the boundedness of $A(x)$ as follows: there exist constants A_{min} and A_{max} such that

$$A_{min} \leq A(x) \leq A_{max} < \mu. \tag{2.3}$$

The BGS are non-zero periodic functions that satisfy the following system

$$\begin{cases} \frac{1}{2}U'' + (\mu - A(x))U - U^3 = 0,\ x \in (0, L), \\ U(0) = U(L),\ U'(0) = U'(L). \end{cases} \tag{2.4}$$

Obviously, $U = 0$ is a trivial solution of system (2.4), but this is not the solution in which we are

interested. Another important fact about the above system is that if $U(x)$ is a solution, then so is $-U(x)$; thus we only study the existence of the positive solution(s).

Here, we seek the existence and uniqueness of the positive BGS through methods from dynamical systems theory. Based on the theory, we first introduce a corresponding parabolic partial differential equation

$$\begin{cases} v_t = \frac{1}{2}v_{xx} + (\mu - A(x))v - v^3, \ x \in (0, L), t > 0, \\ v(0,t) = v(L,t), \ v_x(0,t) = v_x(L,t), \ t \geq 0, \\ v(x,0) = \varphi(x), \ x \in (0,L). \end{cases} \tag{2.5}$$

Next, we present some notations and definitions used in this section. Let $X = \mathcal{C}^{per}([0, L])$ be the set of continuous functions in $(-\infty, \infty)$ and periodic with the prime period L. Its norm is given by the usual supremum norm. Assume P is the positive cone in X, i.e., $P = \{\phi \in X : \phi \geq 0\}$. The interior of P is not empty with a formula $\text{Int}(P) = \{\phi \in X : \phi > 0\}$. For two functions ϕ_1 and ϕ_2 in P, we define $\phi_1 \gg \phi_2$ if $\phi_1 - \phi_2$ is in $\text{Int}(P)$.

Now, let the initial function $\varphi(x)$ in (2.5) be chosen from X and $v(t, x, \varphi)$ be the solution of (2.5). Define a map $\Phi_t(\varphi) = v(t, \cdot, \varphi) : X \to X$ for $t > 0$. Thus, if Φ_t has a unique positive fixed point in P, then (2.5) has a unique positive stationary solution which indicates that (2.4) has a unique positive solution.

Before stating our main theorem, we need the following lemma from [57].

Lemma 2.1. *([57],Theorem 2.3.4) Suppose that $f : P \to P$ is a continuous map. Also assume that*

(1) *f is monotone and strongly subhomogeneous;*

(2) *f is asymptotically smooth, and every positive orbit of f in P is bounded;*

(3) *$f(0) = 0$, and $Df(0)$ is compact and strongly positive.*

Then there exists threshold dynamics:

(a) *If $r(Df(0)) \leq 1$, then every positive orbit in P converges to 0;*

(b) *If $r(Df(0)) > 1$, then there exists a unique fixed point $u^* > 0$ in P such that every positive orbit in $P\backslash\{0\}$ converges to u^*, where $r(Df(0))$ is the spectral radius of $Df(0)$, and $Df(0)$ is the Fréchet derivative of f at zero.*

The definitions of "monotone", "strongly subhomogeneous" and "asymptotically smooth" can be found in [57]. Now we are ready to prove our result.

Our main result is the following theorem.

Theorem 2.2. *(2.4) has a unique positive periodic solution $U(x)$ satisfying $\sqrt{\mu - A_{max}} \leq U(x) \leq \sqrt{\mu - A_{min}}$.*

Proof. Denote $f(\varphi) = \Phi_t(\varphi)$ for any $t > 0$. We want to use the above lemma to prove the existence and the uniqueness of the positive solution to (2.4). Since the diffusion coefficient is a constant $\frac{1}{2}$, it is easy to know that f is a compact operator in X. To verify the other conditions, we divide our proof into the following four steps.

Step 1 Prove that every forward orbit of $f(\varphi)$ is bounded. Choose $\varphi \in P$ and then $\underline{v} = 0$ is a lower solution of Equation (2.5). Similarly, let $\overline{v} = M$ where the constant M satisfies $M \geq \sqrt{\mu - A_{min}}$ and $M > ||\varphi||$. Then we have $\overline{v}_t = 0 \geq (\mu - A(x))M - M^3 = M(\mu - A(x) - M^2)$. So $\overline{v} = M$ is an upper solution of Equation (2.5). Thus by the comparison principle, we have the conclusion that every forward orbit of f is bounded. Since M can be arbitrarily large, from now on we assume the initial functions satisfying $0 \leq \varphi \leq M$, i.e., $\varphi \in [0, M]$.

Step 2 Prove the monotonicity of $f(\varphi)$, that is, we want to prove: if $\varphi_1 \leq \varphi_2$ with $\varphi_1, \varphi_2 \in [0, M] \subset P$, then $f(\varphi_1) \leq f(\varphi_2)$. To this end we rewrite the original system (2.5) as

$$\begin{cases} v_t = \frac{1}{2} v_{xx} - kv + (k + \mu - A(x) - v^2)v, \ x \in (0, L), \ t > 0, \\ v(0, t) = v(L, t), \ v_x(0, t) = v_x(L, t), \ t \geq 0, \\ v(x, 0) = \varphi(x), \ x \in (0, L). \end{cases} \tag{2.6}$$

Denote $\tilde{F}(v) = (k + \mu - A - v^2)v$ and k is a positive large enough real number such that $\tilde{F}_v > 0$, $\forall v \in [0, M] \subset P$. To solve the above system in terms of Green's function, we first find solution of the corresponding homogeneous system. The homogeneous system is

$$\begin{cases} v_t = \frac{1}{2} v_{xx} - kv, \ x \in (0, L), \ t > 0, \\ v(0, t) = v(L, t), \ v_x(0, t) = v_x(L, t), \\ v(x, 0) = \varphi(x), \ x \in (0, L), \end{cases} \tag{2.7}$$

whose solution can be expressed in a formula by way of its Green's function. In view of the separation of variables, the Green's function G has a formula

$$\begin{aligned} G(x, x_0, t) &= \frac{2}{L} \sum_{n=0}^{\infty} e^{-\lambda_n t} \left[\cos\left(\frac{2n\pi x}{L}\right) \cos\left(\frac{2n\pi x_0}{L}\right) + \sin\left(\frac{2n\pi x}{L}\right) \sin\left(\frac{2n\pi x_0}{L}\right) \right], \\ G(x, x_0, t, t_0) &= \frac{2}{L} \sum_{n=0}^{\infty} e^{-\lambda_n (t - t_0)} \left[\cos\left(\frac{2n\pi x}{L}\right) \cos\left(\frac{2n\pi x_0}{L}\right) + \sin\left(\frac{2n\pi x}{L}\right) \sin\left(\frac{2n\pi x_0}{L}\right) \right], \end{aligned}$$

where $\lambda_n = \frac{1}{2}(\frac{2n\pi}{L})^2 + k$ and $n = 0, 1, 2, \cdots$. Thus the solution of the system (2.7) can be written as

$$v(x, t) = G(x, x_0, t) * \varphi(x_0), \tag{2.8}$$

where $*$ denotes the convolution, i.e.,

$$G(x, x_0, t) * \varphi(x_0) = \int_0^L G(x, x_0, t) \cdot \varphi(x_0) dx_0.$$

Here for the Green's function, by the well–known comparison principle, we know that the Green's function is a monotone operator, i.e. $G(x, x_0, t) * \varphi_1(x_0) \leq G(x, x_0, t) * \varphi_2(x_0)$ when

$\varphi_1(x_0) \le \varphi_2(x_0)$. Moreover, we obtain the solution of Equation (2.6) as

$$v(x,t) = G(x,x_0,t) * \varphi(x_0) + \int_0^t G(x,x_0,t,t_0) * \tilde{F}(v(t_0,x_0),x_0)dt_0. \tag{2.9}$$

Now, we consider two cases: $v(x,t)$ is the solution of (2.6) with initial data $\varphi_1(x)$; $\tilde{v}(x,t)$ is the one with $\varphi_2(x)$ as its initial condition. Furthermore, we require $\varphi_1(x) \le \varphi_2(x),\ x \in [0,L]$. Then by Equation (2.9) we will have following formulas

$$v(x,t) = G(x,x_0,t) * \varphi_1(x_0) + \int_0^t G(x,x_0,t,t_0) * \tilde{F}(v(x_0,t_0),x_0)dt_0, \tag{2.10}$$

$$\tilde{v}(x,t) = G(x,x_0,t) * \varphi_2(x_0) + \int_0^t G(x,x_0,t,t_0) * \tilde{F}(\tilde{v}(x_0,t_0),x_0)dt_0. \tag{2.11}$$

As we already know that the Green's function is a monotone operator, it is easy to derive $v(x,t) \le \tilde{v}(x,t)$ when $\varphi_1 \le \varphi_2$.

Step 3 Prove that $f(\varphi)$ is strongly sub-homogeneous, that is, $f(\lambda\varphi) \gg \lambda f(\varphi)$ when $\varphi \gg 0$ and $\lambda \in (0,1)$. Now, we take $v(x,t)$ as a solution of Equation (2.5) corresponding to the initial function φ, while $\tilde{v}(x,t)$ is a solution corresponding to the initial function $\lambda\varphi$. Since the nonlinear function $(\mu - A(x))v - v^3$ is sub-homogeneous, i.e.,

$$(\mu - A(x))(\lambda v) - (\lambda v)^3 > \lambda[(\mu - A(x))v - v^3]$$

for $v \gg 0$ and $\lambda \in (0,1)$, we can use (2.9) to derive that $\tilde{v} \gg \lambda v$, i.e., $f(\lambda\varphi) \gg \lambda f(\varphi)$.

Step 4 The last step is to prove that the solution $v = 0$ is unstable. Actually, in system (2.5) if $\varphi = 0$, then $v = 0$ for all $t \ge 0$, that is $f(0) = 0$. Thus we linearize the system (2.5) around $v = 0$, giving

$$v_t \ = \ \frac{1}{2}v_{xx} + (\mu - A(x))v.$$

Consider the system

$$\begin{cases} \bar{v}_t = \frac{1}{2}\bar{v}_{xx} + (\mu - A_{max})\bar{v},\ x \in (0,L),\ t > 0, \\ \bar{v}(0,t) = \bar{v}(L,t),\ \bar{v}'(0,t) = \bar{v}'(L,t),\ t \ge 0, \\ \bar{v}(x,0) = \varphi(x). \end{cases} \tag{2.12}$$

Let $\bar{v}(x,t) = X(x)e^{\lambda t}$. Substituting it into the above equation gives

$$\lambda X = \frac{1}{2}X'' + (\mu - A_{max})X.$$

From the boundary condition, we have

$$\lambda_n = -2\left(\frac{n\pi}{L}\right)^2 + \mu - A_{max},\ n = 0, 1, 2, \cdots .$$

Clearly, the principal eigenvalue of the system (2.12) is $\lambda_0 = \mu - A_{max} > 0$. Thus by comparison, we have the result that $v = 0$ is an unstable equilibrium for (2.5) .

Based on above arguments, by Lemma 5.1, we arrive at the first part of our theorem. Furthermore, from Step 1, it is easy to have $U(x) \leq \sqrt{\mu - A_{min}}$; on the other hand, taking $\underline{v} = \sqrt{\mu - A_{max}}$ gives $\underline{v}_t = 0 \leq (A_{max} - A(x))(\mu - A_{max})$, by comparison, which implies $\sqrt{\mu - A_{max}}$ is also a lower solution of Equation (2.5). Thus, $\sqrt{\mu - A_{max}} \leq U(x) \leq \sqrt{\mu - A_{min}}$. ∎

Remark 2.3. *The positive solution $U(x)$ found in Theorem 2.1 corresponds to $U_+(x)$ in Equation (1.12), meanwhile, $U_-(x)$ corresponds to the negative solution $-U(x)$.*

The DSS is a heteroclinic orbit connecting the periodic solutions $U_+(x)$ and $U_-(x)$. The existence of the DSS can be proved by the combination of several techniques from the classical theory of ordinary differential equations and the dynamics of planar homomorphisms. The details are shown in [48] with the corresponding parameters "$g_1 = 1$" and "$g_2 = 0$". Thus, we will concentrate on finding the asymptotic behavior of the DSS when $x \to \pm\infty$. Indeed, we only consider the case near the far-field $x = +\infty$, since the analysis near $x = -\infty$ is similar. We assume

$$\Phi(x) \sim U(x) + \delta\phi(x)e^{-\beta x},\ x \to +\infty,\ \beta \geq 0, \tag{2.13}$$

where $U(x)$ is the positive background solution in Theorem 2.1. Now, we substitute (2.13) into Equation (2.2) to get

$$O(\delta^1): \quad \frac{1}{2}\phi'' - \beta\phi' + \left[\frac{1}{2}\beta^2 + \mu - A(x) - 3U^2\right]\phi = 0. \tag{2.14}$$

Denote

$$L_\beta = \frac{1}{2}\frac{d^2}{dx^2} - \beta\frac{d}{dx} + \left[\frac{1}{2}\beta^2 + \mu - A(x) - 3U^2\right],$$

so the problem is to find the non-zero solution of $L_\beta\phi = 0$. Let λ be the principal (largest) eigenvalue of the operator and we consider the following eigenvalue problem

$$L_\beta\phi = \lambda\phi, \quad \phi(x) = \phi(x + L), \quad x \in [0, L], \tag{2.15}$$

for some periodic and positive function $\phi(x)$. Thus, the problem (2.14) can be viewed as to find the eigenfunction of (2.15) corresponding to $\lambda = 0$. It is easy to see that the principal eigenvalue λ depends on the parameter β, so we use $\lambda(\beta)$ to identify their relationship in the following context. In fact, we have the following observations.

(1) When $\beta \to +\infty$, we will have $\frac{1}{2}\beta^2 + \mu - A(x) - 3U^2 > 0$. By comparison, we obtain $\lambda(+\infty) > 0$.

(2) When $\beta = 0$, the eigenvalue problem becomes

$$L_0\phi = \frac{1}{2}\phi'' + [\mu - A(x) - 3U^2]\phi = \lambda(0)\phi,\ \phi(x) = \phi(x+L). \tag{2.16}$$

If $\lambda(0) < 0$, by the continuity of the principal eigenvalue, there should exist at least one β^* in the interval $(0, +\infty)$, such that $\lambda(\beta^*) = 0$ and the corresponding eigenfunction ϕ_{β^*} is the solution to Equation (2.14).

Next, we are going to show the uniqueness of β if $\lambda(0) < 0$.

Proposition 2.4. *The principal eigenvalue $\lambda(\beta)$ defined in (2.15) is convex with respect to $\beta \geq 0$.*

Proof. Convexity means

$$\lambda\left(\frac{\beta_1+\beta_2}{2}\right) \leq \frac{\lambda(\beta_1)+\lambda(\beta_2)}{2}, \quad \beta_1, \beta_2 > 0.$$

Assume that $\lambda(\frac{\beta_1+\beta_2}{2})$ is the principal eigenvalue of $L_{\frac{\beta_1+\beta_2}{2}}$ satisfying

$$L_{\frac{\beta_1+\beta_2}{2}}\tilde{\phi} = \lambda\left(\frac{\beta_1+\beta_2}{2}\right)\tilde{\phi},$$

where $\tilde{\phi}$ is positive and L-periodic. Then we need to prove

$$L_{\frac{\beta_1+\beta_2}{2}}\tilde{\phi} \leq \frac{\lambda(\beta_1)+\lambda(\beta_2)}{2}\tilde{\phi},$$

where $\lambda(\beta_1)$ and $\lambda(\beta_2)$ satisfy

$$L_{\beta_1}\phi \leq \lambda(\beta_1)\phi, \quad L_{\beta_2}\phi \leq \lambda(\beta_2)\phi,$$

for any positive and L-periodic ϕ. On the other hand, from the definition of $L_\beta\phi$ and convexity of β^2, we have

$$\begin{aligned}
L_{\frac{\beta_1+\beta_2}{2}}\tilde{\phi} &= \frac{1}{2}\left(\tilde{\phi}'' - 2\frac{\beta_1+\beta_2}{2}\tilde{\phi}'\right) + \left[\frac{1}{2}\left(\frac{\beta_1+\beta_2}{2}\right)^2 + (\mu - A(x) - 3U^2)\right]\tilde{\phi} \\
\leq\ & \frac{1}{2}\left(\tilde{\phi}'' - \beta_1\tilde{\phi}' - \beta_2\tilde{\phi}'\right) + \frac{1}{2}\left(\frac{1}{2}\beta_1^2 + \frac{1}{2}\beta_2^2\right)\tilde{\phi} + \frac{1}{2}\left[2\left(\mu - A(x) - 3U^2\right)\right]\tilde{\phi} \\
=\ & \frac{1}{2}[L_{\beta_1}\tilde{\phi} + L_{\beta_2}\tilde{\phi}] \\
\leq\ & \frac{1}{2}(\lambda(\beta_1) + \lambda(\beta_2))\tilde{\phi}.
\end{aligned}$$

This proves the convexity of $\lambda(\beta)$. ∎

Combining the above proposition and the continuity of L_β on β, we have the following conclusion.

Theorem 2.5. *If $\lambda(0) < 0$, then there exists only one $\beta = \beta^*$ such that $\lambda(\beta^*) = 0$.*

The value of $\beta = \beta^*$ can be obtained numerically from the principal eigenvalue of (2.15) with $\lambda = 0$. In [30, 31], the authors used a variational structure to find the approximate value for β and their results on β are only accurate for some special potential functions.

Remark 2.6. *By Theorem 2.2, we know that $\mu - A_{max} \leq U^2$ and it is easy to verify that $3A_{max} - A_{min} - 2\mu < 0$ is a sufficient condition for $\lambda(0) < 0$.*

2.2 Stability/Instability

In this section, we study the linear stability/instability of the stationary solutions for both the BGS and the DSS cases. To do this, we follow the standard approach in references [25, 31] and consider a perturbation of the stationary solution with the following form

$$V(x, y, t) = v(x) + \delta(u_1(x) + iu_2(x))e^{\lambda t}e^{imy} + \delta(u_1^*(x) + iu_2^*(x))e^{\lambda^* t}e^{-imy}, \tag{2.17}$$

where $v(x)$ is a stationary solution containing the BGS or the DSS, i denotes the imaginary unit, $*$ represents the complex conjugation, δ is a small parameter, λ is an eigenvalue, $u = (u_1, u_2)^T$ is the corresponding eigenfunction and m is the corresponding wave number along the y direction.

We start with the stability of the BGS by assuming $v(x)$ to be the positive BGS $U(x)$. Thus, by substituting Equation (2.17) into Equation (1.10) (in views of the linear independence of $e^{\lambda t}e^{imy}$ and $e^{\lambda^* t}e^{-imy}$), we find the eigenvalue problem as follows

$$\begin{cases} -\frac{1}{2}u_1'' + \frac{1}{2}m^2u_1 + (A(x) - \mu)u_1 + 3U^2u_1 = -\lambda u_2, \\ -\frac{1}{2}u_2'' + \frac{1}{2}m^2u_2 + (A(x) - \mu)u_2 + U^2u_2 = \lambda u_1. \end{cases} \tag{2.18}$$

Equation (2.18) can be rewritten in a matrix form

$$Lu + \frac{1}{2}m^2Iu = \lambda Ju, \tag{2.19}$$

where

$$u = \begin{pmatrix} u_1 \\ u_2 \end{pmatrix},\ L = \begin{pmatrix} L_+ & 0 \\ 0 & L_- \end{pmatrix},\ I = \begin{pmatrix} 1 & 0 \\ 0 & 1 \end{pmatrix},\ J = \begin{pmatrix} 0 & -1 \\ 1 & 0 \end{pmatrix}, \tag{2.20}$$

and

$$L_+ \ = \ -\frac{1}{2}\frac{d^2}{dx^2} + (A(x) - \mu) + 3U^2,$$

$$L_- = -\frac{1}{2}\frac{d^2}{dx^2} + (A(x) - \mu) + U^2.$$

It is well-known that the eigenvalue λ depends on the eigenfunction space that is chosen. Here for the eigenfunction, we confine to a specific weighted functional space, i.e., we want to find the eigenvalues for eigenfunctions satisfying

$$e^{\alpha x}(u_1, u_2) \text{ is bounded for } x \in (-\infty, \infty) \tag{2.21}$$

for some real constant α. In other words, we look for eigen solution with the following form

$$\begin{pmatrix} u_1 \\ u_2 \end{pmatrix} = \begin{pmatrix} f_1(x)e^{\alpha x} \\ f_2(x)e^{\alpha x} \end{pmatrix} \tag{2.22}$$

for some bounded functions $f_1,\ f_2$ and real number α. For mathematical detail and physical implication of this approach, we refer readers to [44, 49] and the references therein. Obviously the spectral problem is dependent on the choice of α. For a particular choice of real α, see [25] (they used a weight function e^{iqx} with $q = 2i$ or i).

First, we assume that f_1, f_2 are non-zero L-periodic functions, i.e., $f_j(x) = f_j(x + L) \not\equiv 0,\ j = 1, 2$. In other words, f_1 and f_2 are in $X = \mathcal{C}^{per}([0, L])$, the set of all continuous functions in $(-\infty, \infty)$ and periodic with the prime period L. We substitute (2.22) into Equation (2.18) to get

$$L_\alpha f + \frac{1}{2}\left(m^2 - \alpha^2\right) If = \lambda J f, \tag{2.23}$$

where

$$f = \begin{pmatrix} f_1 \\ f_2 \end{pmatrix},\ L_\alpha = \begin{pmatrix} L_\alpha^+ & 0 \\ 0 & L_\alpha^- \end{pmatrix},$$

and

$$\begin{aligned} L_\alpha^+ &= -\frac{1}{2}\frac{d^2}{dx^2} - \alpha\frac{d}{dx} + (A(x) - \mu) + 3U^2, \\ L_\alpha^- &= -\frac{1}{2}\frac{d^2}{dx^2} - \alpha\frac{d}{dx} + (A(x) - \mu) + U^2. \end{aligned}$$

Here I and J are defined in Equation (2.20).

It is not easy to solve the whole spectral problem. First we are only concerned with the existence of the critical eigenvalue, i.e. $\lambda = 0$. By assuming $\lambda = 0$ in (2.23), the problem reduces to

$$\begin{cases} \left[L_\alpha^+ + \frac{1}{2}\left(m^2 - \alpha^2\right)\right] f_1 = 0, \\ \left[L_\alpha^- + \frac{1}{2}\left(m^2 - \alpha^2\right)\right] f_2 = 0. \end{cases} \tag{2.24}$$

The above problem becomes decoupled and it is able to find the corresponding eigenfunctions for suitable choice of m. To investigate the above problem, we first assume that k_1 and k_2 (in

fact, $k_1(\alpha)$ and $k_2(\alpha)$) are the principal (smallest) eigenvalues of

$$\begin{cases} L_\alpha^+ g_1 = k_1 g_1, \\ L_\alpha^- g_2 = k_2 g_2, \end{cases} \tag{2.25}$$

with periodic eigenfunctions g_1 and g_2 respectively. By comparison, we know $k_1 > k_2$, due to the fact that $L_\alpha^+ = L_\alpha^- + 2U^2$. Then returning to (2.24), we get two critical numbers m_1 and m_2. Here m_1 is given by

$$m_1 = \sqrt{\alpha^2 - 2k_1}, \tag{2.26}$$

so that (2.23) has a solution $\lambda = 0$ with $f_1 = g_1, f_2 = 0$. Similarly m_2 is given by

$$m_2 = \sqrt{\alpha^2 - 2k_2}, \tag{2.27}$$

so that (2.23) has a solution $\lambda = 0$ with $f_1 = 0, f_2 = g_2$.

Obviously we have $m_2 > m_1$ if both of them are real (i.e., $\alpha^2 - 2k_1 \geq 0$). By (2.14), a particular choice of $\alpha = -\beta$ with $\beta = \beta^*$ in Theorem 2.5 will yield $k_1 = \frac{1}{2}\alpha^2,\ m_1 = 0,\ m_2 > 0$.

We now give a further analysis on the eigenvalue of (2.23) when $m_1 < m < m_2$.

Combining two equations in (2.23), we get

$$\left(L_\alpha^+ + \frac{1}{2}\left(m^2 - \alpha^2\right)\right)\left(L_\alpha^- + \frac{1}{2}\left(m^2 - \alpha^2\right)\right) f_2 = -\lambda^2 f_2.$$

When $m_1 < m < m_2$, we have that every eigenvalue of $L_\alpha^+ + \frac{1}{2}\left(m^2 - \alpha^2\right)$ is positive. Thus it is invertible. By [25], we get

$$-\lambda^2 = \min \frac{\langle f_2, (L_\alpha^- + \frac{1}{2}\left(m^2 - \alpha^2\right)) f_2 \rangle}{\langle f_2, (L_\alpha^+ + \frac{1}{2}\left(m^2 - \alpha^2\right))^{-1} f_2 \rangle}, \tag{2.28}$$

where

$$\langle g_1, g_2 \rangle = \int_0^L g_1 \bar{g}_2 dx.$$

Now, if we choose $f_2 = g_2$ to be the principal eigenfunction corresponding to $L_\alpha^- g_2 = k_2 g_2$ in Equation (2.25), then $f_2 > 0$. Thus, $\left\langle f_2, (L_\alpha^+ + \frac{1}{2}\left(m^2 - \alpha^2\right))^{-1} f_2 \right\rangle$ is positive because of $m_1 < m$; on the other hand, $\left(L_\alpha^- + \frac{1}{2}\left(m^2 - \alpha^2\right)\right) f_2 = \delta f_2$ for some $\delta < 0$ due to the fact $m < m_2$. Obviously, by Equation (2.28), we find that there exists at least one eigenvalue satisfying $\Re(\lambda) > 0$ when $m_1 < m < m_2$.

Furthermore, if $f_1(x)$ and $f_2(x)$ are not L-periodic, but in $L^2(-\infty, \infty)$. Then by the Floquet–Bloch theory [49], we let

$$f_j(x) = \hat{f}_j(x) e^{i\eta x},\ \hat{f}_j(x) = \hat{f}_j(x + L),\ j = 1, 2, \tag{2.29}$$

where $\eta \in [-\frac{\pi}{L}, \frac{\pi}{L}]$ is called the Bloch wavenumber. Substituting Equation (2.29) into Equation

(2.23) gives

$$L_{\alpha,\eta}\hat{f} + \frac{1}{2}\left[m^2 - (\alpha + i\eta)^2\right] I\hat{f} = \lambda J\hat{f}, \tag{2.30}$$

where

$$\hat{f} = \begin{pmatrix} \hat{f}_1 \\ \hat{f}_2 \end{pmatrix}, \; L_{\alpha,\eta} = \begin{pmatrix} L^+_{\alpha,\eta} & 0 \\ 0 & L^-_{\alpha,\eta} \end{pmatrix},$$

and

$$\begin{aligned} L^+_{\alpha,\eta} &= -\frac{1}{2}\frac{d^2}{dx^2} - (\alpha + i\eta)\frac{d}{dx} + (A(x) - \mu) + 3U^2, \\ L^-_{\alpha,\eta} &= -\frac{1}{2}\frac{d^2}{dx^2} - (\alpha + i\eta)\frac{d}{dx} + (A(x) - \mu) + U^2. \end{aligned}$$

By formula (4.18) in [49], the spectrum of (2.23) is the union over all $\eta \in [-\frac{\pi}{L}, \frac{\pi}{L}]$ of the point spectra of (2.30). This includes the point spectra when $\eta = 0$. Thus, when $m_1 < m < m_2$, we can find at least one eigenvalue λ satisfying $\Re(\lambda) > 0$.

To illustrate the stability analysis, we give a simple constant example in Appendix A, i.e., $A(x) \equiv A$ for all $x \in \mathbb{R}$ to verify our analysis. Due to the constant potential, we can compute all the eigenvalues and manifest the relationship between $\Re(\lambda)$ and $\Im(\lambda)$.

For the linear stability of the DSS, we take $v(x)$ in Equation (2.17) as the DSS $\Phi(x)$. After substituting and simplifying, we find the eigenvalue problem as

$$\begin{cases} -\frac{1}{2}u_1'' + \frac{1}{2}m^2 u_1 + (A(x) - \mu)u_1 + 3\Phi^2 u_1 = -\lambda u_2, \\ -\frac{1}{2}u_2'' + \frac{1}{2}m^2 u_2 + (A(x) - \mu)u_2 + \Phi^2 u_2 = \lambda u_1. \end{cases} \tag{2.31}$$

When incorporating the weighted functional space and using the setting of (2.22), similarly we have

$$\begin{cases} -\frac{1}{2}f_1'' - \alpha f_1' - \frac{1}{2}\alpha^2 f_1 + \frac{1}{2}m^2 f_1 + (A(x) - \mu)f_1 + 3\Phi^2 f_1 = -\lambda f_2, \\ -\frac{1}{2}f_2'' - \alpha f_2' - \frac{1}{2}\alpha^2 f_2 + \frac{1}{2}m^2 f_2 + (A(x) - \mu)f_2 + \Phi^2 f_2 = \lambda f_1. \end{cases} \tag{2.32}$$

In the above system, we notice that near $x = \pm\infty$, the eigenvalue problem reduces to the exact eigenvalue problem of the BGS. This is because $\Phi(x) - U_+(x) \to 0$ as $x \to +\infty$ and $\Phi(x) - U_-(x) \to 0$ as $x \to -\infty$. By using the theory of [16], we can obtain the essential spectrum of the above system by using the results of system (2.23).

2.3 Numerical simulations

In this section, we will carry out numerical simulations on the global dynamics of the system. We choose the external potential as the form $A(x) = V_0 \cos^2(kx)$. Throughout all the simulations, the chemical potential and the frequency of the optical lattice are fixed as $\mu = 1.05$ and $k = 1$ respectively.

α	m_1	m_2
-1.6	0.4565	1.5885
-2.0	1.2839	1.9898
-2.5	1.9744	2.4912

Table 2.1: Critical numbers of m vs. α. The above table corresponds to the parameter set: $\mu = 1.05$ and $A(x) = \cos^2(x)$.

First, we numerically obtain the stationary solutions (including the BGS and the DSS) for (1.10) by using the Newton's method. By substituting an L-periodic function as an initial guess for the BGS (a hyperbolic tangent function is taken as an initial guess for the DSS), we can get the result Figure 1.1 shown in the introduction. As seen in the figure, the BGS is a L-periodic function and the DSS is a heteroclinic solution which connects the positive BGS and the negative BGS.

Secondly, we numerically demonstrate the stability/instability for the stationary solutions. Here, we consider three cases: (a) fixed V_0 with varying α; (b) fixed α with varying V_0; (c) the transverse modulational instability.

To investigate case (a), we shall indicate the relationship between the critical wave numbers and α. The strength of the OL is chosen as $V_0 = 1$. The computation is carried out in the interval of $x \in [-2\pi, 2\pi]$. By applying the central finite difference on the eigenvalue problem (2.25) with periodic boundary conditions, i.e., $g_j(-L) = g_j(L),\ g_j'(-L) = g_j'(L),\ j = 1, 2,\ L = 2\pi$, and following the formulas (2.26) and (2.27), we obtain the critical wave numbers shown in Table 2.1. Based on the table, for each value of α, we then choose some appropriate m between the two corresponding critical numbers (namely in the unstable regime), and find out that the real part of the principal eigenvalue is larger than zero. The details are shown in Figure 2.1. From the figure, it also can be seen that the curve shifts to right as α decreases.

To investigate case (b), we shall numerically derive the relationship between the critical wave numbers and the strength of the OL V_0. The magnitude of α is chosen to be relatively large as $\alpha = -2.5$. By the same numeric method and boundary conditions used in case (a), we obtain Table 2.2 and Figure 2.2. From the table, it is easy to have that the minimal critical wavenumber m_1 decreases when the value of V_0 decreases. Furthermore, as shown in the figure, the value of $\Re(\lambda)$ increases as V_0 decreases, which implies the instability becomes stronger.

To investigate case (c), we need to analyze the transverse modulational instability of the dark soliton stripe in the presence of the OL. We do the simulations on the BGS ($U(x, y, t)$) and the DSS ($v(x, y, t)$) simultaneously. We apply the central finite difference on the space variables and the fourth-order Runge-Kutta method (RK4) on the time variable of Equation (1.10); for the boundary condition, we use the Neumann boundary condition along x direction, that is, $v'(-L, y, t) = v'(L, y, t) = 0$ as well as $U'(-L, y, t) = U'(L, y, t) = 0$, $L = 20$. We start with the stationary solutions with an added random perturbation of relative size 10^{-5}. Figures 2.3 and 2.4 show the details. To be clear, the simulations in these figures are performed in the domain of

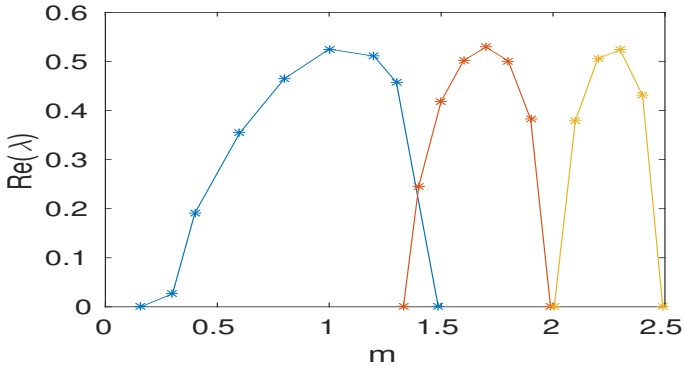

Figure 2.1: (Color online) The principal eigenvalue of (2.23) vs. m. Parameters corrspond to the set: $\mu = 1.05$ and $A(x) = \cos^2(x)$. Those three curves correspond to different values of α. The leftmost (blue) curve corresponds to $\alpha = -1.6$, the middle (red) curve corresponds to $\alpha = -2$ and the rightmost (yellow) curve corresponds to $\alpha = -2.5$.

V_0	m_1	m_2
1.0	1.9744	2.4912
0.5	1.7383	2.4983
0	1.4318	2.5
-0.5	1.0169	2.4990
-1.0	0.0593	2.4968

Table 2.2: Critical numbers of m vs. V_0. The above table corrosponds to the parameter set: $\mu = 1.05$, $\alpha = -2.5$ and $A(x) = V_0 \cos^2(x)$.

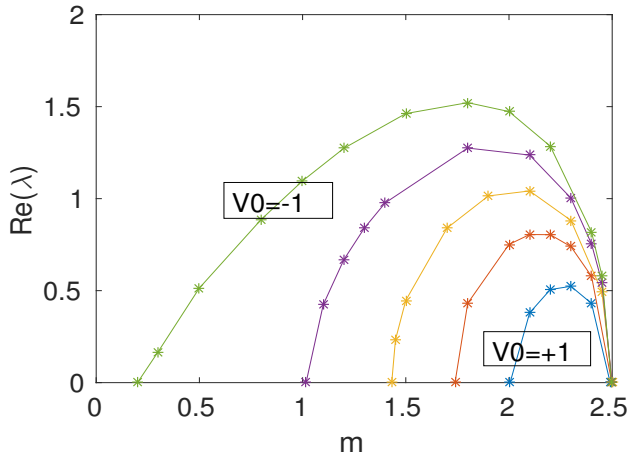

Figure 2.2: (Color online) The principal eigenvalue of (2.23) vs. m. Parameters correspond to the set: $\mu = 1.05$, $\alpha = -2.5$ and $A(x) = V_0 \cos^2(x)$. Different curves correspond to different values of V_0. From top to bottom, the curves correspond to $V_0 = -1$, $V_0 = -0.5$, $V_0 = 0$, $V_0 = 0.5$ and $V_0 = 1$ respectively.

$(x, y) \in [-20, 20] \times [-20, 20]$; the figures show density snapshots at a period of time, where the density means the DSS's density ($|v|^2$) divided by the BGS's ($|U|^2$), that is, $|v|^2/|U|^2$. Comparing these figures, we have the following observations.

1. When $V_0 \ll \mu$, the DSS will evolve into vortices. When the value of V_0 decreases, the DSS evolves into vortices earlier. As shown in these figures, clear vortices occur at time $t \simeq 40$ when $V_0 = 0.2$, and $t \simeq 30$ when $V_0 = -1$.

2. When $0 < V_0$, after a period of time, the DSS will oscillate horizontally along x direction to exhibit a snake-like instability, as shown in Figure 2.3.

These observations coincide with the results in case (b): when V_0 decreases, the instability happens earlier and stronger.

Lastly, we shall give an example to illustrate the relationship between $\Re(\lambda)$ and $\Im(\lambda)$. The same numeric scheme and periodic boundary conditions as in case (a) are used here. In Figure 2.5, we choose $\alpha = -2$ and $m = 1.5$ which is in the unstable regime. As presented in the figure, the minimal value of nonnegative $\Re(\lambda)$ is away from zero, which agrees with the stability analysis in the Appendix 5.2 for the case of constant potential.

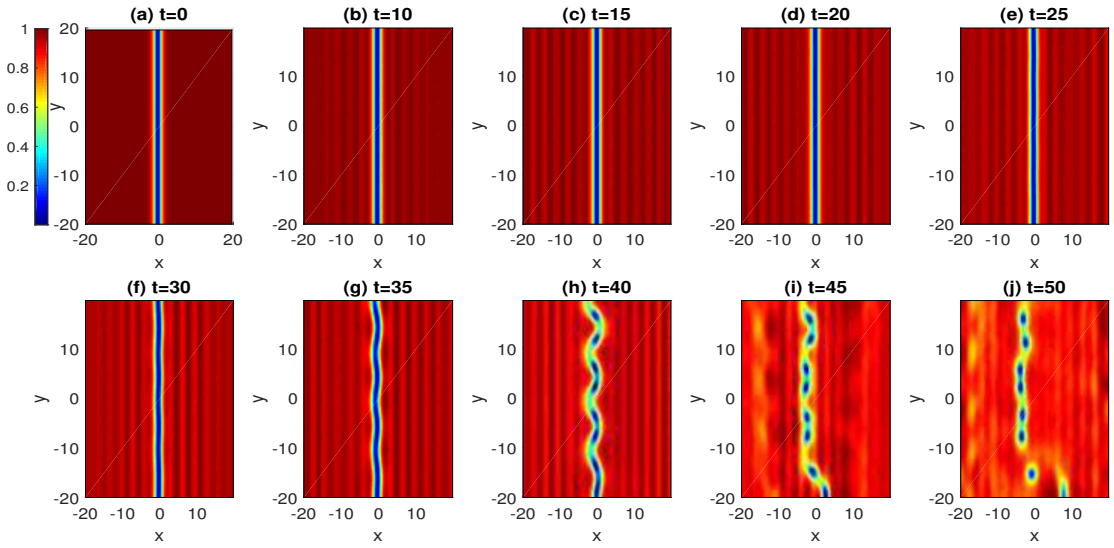

Figure 2.3: (Color online) The dynamics when $V_0 = 0.2$.

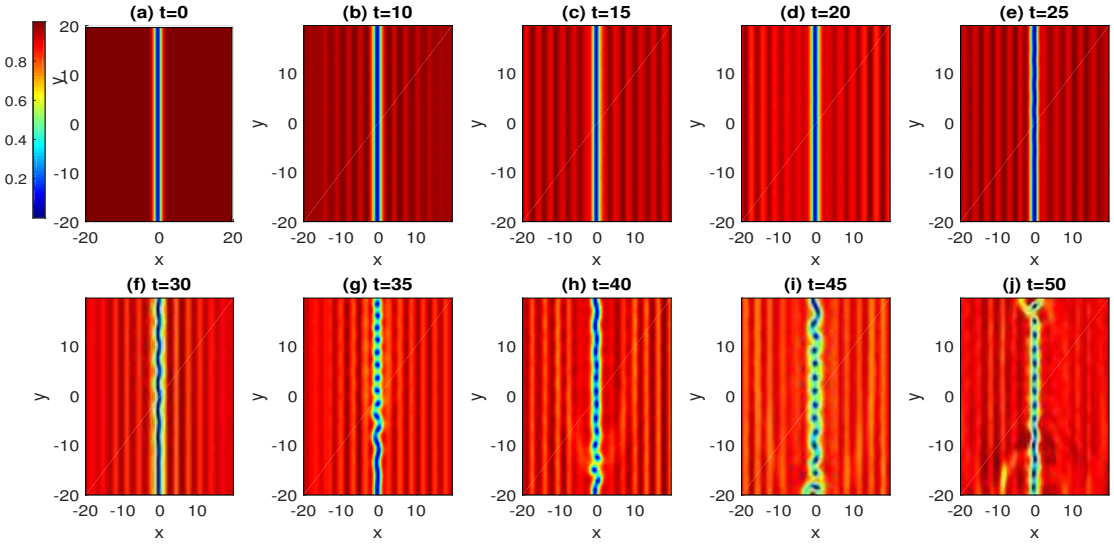

Figure 2.4: (Color online) The dynamics when $V_0 = -1$.

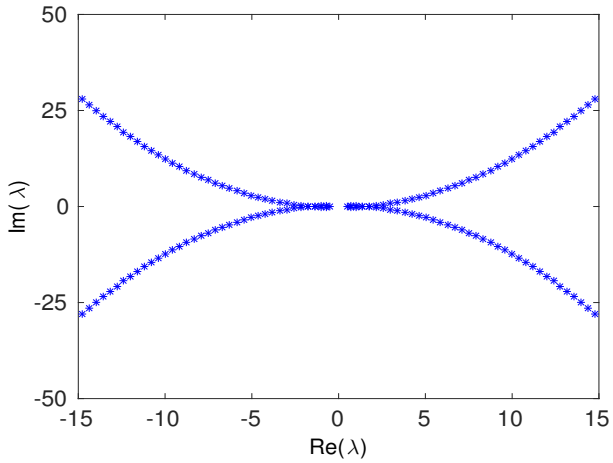

Figure 2.5: (Color online) The eigenvalues of the BGS. Parameters correspond to the set: $\mu = 1.05$, $A(x) = \cos^2(x)$, $\alpha = -2$ and $m = 1.5$.

Chapter 3

Dynamics for large chemical potential

In this chapter, we consider the case when the chemical potential μ is relatively large compared to the magnitude of $A(x)$ and the DSS. Now, we start from the following equation

$$iv_t = -\frac{1}{2}(v_{xx} + v_{yy}) + (A(x) - \mu)v + |v|^2 v,\ x \in \mathbb{R},\ y \in (-\pi, \pi). \tag{3.1}$$

Because of the assumption $\mu \gg 1$, we need to rescale the above equation. Dividing μ on both sides yields

$$i\frac{v_t}{\mu} = \frac{1}{2}\left(\frac{v_{xx}}{\mu} + \frac{v_{yy}}{\mu}\right) + \left(\frac{A(x)}{\mu} - 1\right)v + \frac{|v|^2 v}{\mu}. \tag{3.2}$$

Let

$$v = \sqrt{\mu}\overline{v}, \tag{3.3}$$

and thus

$$i\frac{\overline{v}_t}{\mu} = \frac{1}{2}\left(\frac{\overline{v}_{xx}}{\mu} + \frac{\overline{v}_{yy}}{\mu}\right) + \left(\frac{A(x)}{\mu} - 1\right)\overline{v} + |\overline{v}|^2\overline{v}. \tag{3.4}$$

To simplify the above equation, we let

$$\epsilon = \frac{1}{\mu},\quad \overline{t} = \mu t,\quad w(x, y, \overline{t}) = \overline{v}(x, y, \overline{t}). \tag{3.5}$$

Finally, we get our rescaled equation as follows

$$iw_{\overline{t}} = -\frac{1}{2}\epsilon(w_{xx} + w_{yy}) + (\epsilon A(x) - 1)w + |w|^2 w, \tag{3.6}$$

where ϵ is a small parameter.

In the following sections, we investigate the existence and linear stability of the stationary solution of the above equation by means of asymptotic analysis.

3.1 Asymptotic analysis of the stationary solutions

To investigate the existence of the BGS and the DSS, we will use asymptotic analysis to find the formulas of the stationary solutions of Equation (3.6). As discussed in the introduction, it is reasonable to assume that the solution is homogeneous in y direction. Thus, our aim is to find the solutions to the following equation

$$-\frac{\epsilon}{2}w_{xx} + (\epsilon A(x) - 1)w + w^3 = 0. \tag{3.7}$$

It is easy to verify that if w is a solution, then so is $-w$. This fact leads us to mainly be concerned with the positive solution in the following context.

An exploiting fact is that if ϵ is a small parameter, we can expand the outer solution (the BGS) as follows

$$w = w_0 + \epsilon w_1 + \epsilon^2 w_2 + \cdots . \tag{3.8}$$

Substituting (3.8) into (3.7) and rearranging them in powers of ϵ yields a series of equations. The details are given as follows.

Up to $\mathcal{O}(\epsilon^0)$, we have

$$\begin{cases} -w_0 + w_0^3 = 0, \\ w_0(x) = w_0(x + L). \end{cases} \tag{3.9}$$

Here, we need to exclude the zero solution; otherwise, the whole solution is zero. Therefore, we have

$$w_0(x) = 1. \tag{3.10}$$

Up to $\mathcal{O}(\epsilon^1)$, we get

$$\begin{cases} A(x)w_0 + 2w_1 = 0, \\ w_1(x) = w_1(x + L). \end{cases} \tag{3.11}$$

Solving the above system gives

$$w_1(x) = -\frac{1}{2}A(x). \tag{3.12}$$

Up to $\mathcal{O}(\epsilon^2)$, we obtain

$$\begin{cases} -\frac{1}{2}w_1'' + A(x)w_1 + 3w_0w_1^2 + 2w_2 = 0, \\ w_2(x) = w_2(x + L). \end{cases} \tag{3.13}$$

Solving for w_2 leads to

$$w_2(x) = -\frac{1}{8}[A''(x) + A^2(x)]. \tag{3.14}$$

Thus, we get the asymptotic formula for the positive BGS as

$$w(x) = 1 - \frac{\epsilon}{2}A(x) - \frac{\epsilon^2}{8}[A''(x) + A^2(x)] + \cdots . \tag{3.15}$$

For the DSS, there is a boundary layer near $x = 0$. We will use the boundary theory coupled with matching asymptotics to obtain its asymptotic formula. From the above analysis, by symmetry, we can get the outer solution for the DSS as

$$w(x) = \begin{cases} 1 - \frac{\epsilon}{2}A(x) - \frac{\epsilon^2}{8}[A''(x) + A^2(x)] + \cdots, & x > 0, \\ -1 + \frac{\epsilon}{2}A(x) + \frac{\epsilon^2}{8}[A''(x) + A^2(x)] + \cdots, & x < 0. \end{cases} \tag{3.16}$$

Next we look for the inner solution near $x = 0$ and let

$$z = \frac{x}{\sqrt{\epsilon}}, \ w(x) = w(\sqrt{\epsilon}z) = \bar{w}(z), \ A(x) = A(\sqrt{\epsilon}z), \tag{3.17}$$

to obtain

$$w' = \frac{1}{\sqrt{\epsilon}}\bar{w}', \ w'' = \frac{1}{\epsilon}\bar{w}''.$$

Therefore Equation (3.7) becomes

$$-\frac{1}{2}\bar{w}'' + (\epsilon A(\sqrt{\epsilon}z) - 1)\bar{w} + \bar{w}^3 = 0. \tag{3.18}$$

Clearly, we need to expand the term $\epsilon A(\sqrt{\epsilon}y)$. Using the Taylor expansion, we get

$$\epsilon A(\sqrt{\epsilon}z) = \epsilon A(0) + \epsilon^{\frac{3}{2}}A'(0)z + \cdots.$$

Correspondingly, we expand v as

$$\bar{w} = \bar{w}_0 + \epsilon^{\frac{1}{2}}\bar{w}_1 + \epsilon\bar{w}_2 + \epsilon^{\frac{3}{2}}\bar{w}_3 + \cdots. \tag{3.19}$$

Substituting them into Equation (3.18) yields a series of equations at different orders.

Up to $\mathcal{O}(\epsilon^0)$, we have

$$\begin{cases} -\frac{1}{2}\bar{w}_0'' - \bar{w}_0 + \bar{w}_0^3 = 0, \\ \bar{w}_0(0) = 0. \end{cases} \tag{3.20}$$

The corresponding matching condition is

$$\lim_{z\to+\infty} \bar{w}_0(z) = \lim_{x\to 0^+} w_0 = 1. \tag{3.21}$$

Solving the above system gives

$$\bar{w}_0(z) = \tanh(z), \quad z \geq 0. \tag{3.22}$$

For terms of $\mathcal{O}(\epsilon^{\frac{1}{2}})$, we get

$$\begin{cases} -\frac{1}{2}\bar{w}_1'' - \bar{w}_1 + 3v_0^2\bar{w}_1 = 0, \\ \bar{w}_1(0) = 0. \end{cases} \tag{3.23}$$

The corresponding matching condition is

$$\bar{w}_1(+\infty) = 0. \tag{3.24}$$

From Equation (3.20), we can see that

$$y_1(z) = \bar{w}_0'(z) = \operatorname{sech}^2(z) \tag{3.25}$$

is a solution of Equation (3.23). To find another independent solution $y_2(z)$, we use the method of reduction of order and get

$$y_2(z) = \operatorname{sech}^2(z)\int_0^z \frac{1}{\operatorname{sech}^4(s)}ds = \frac{\operatorname{sech}^2(z)[\sinh(4z) + 8\sinh(2z) + 12z]}{32}. \tag{3.26}$$

Thus, we have the expression for $\bar{w}_1$ as $\bar{w}_1 = c_1y_1 + c_2y_2$. From its boundary condition and the matching condition, it is easy to have $\bar{w}_1 = 0$.

Up to $\mathcal{O}(\epsilon^1)$, we obtain

$$\begin{cases} -\frac{1}{2}\bar{w}_2'' - \bar{w}_2 + 3\bar{w}_0^2\bar{w}_2 + A(0)\bar{w}_0 = 0, \\ \bar{w}_2(0) = 0. \end{cases} \tag{3.27}$$

Now, the corresponding matching condition is

$$\lim_{z\to+\infty} \bar{w}_2(z) = \lim_{x\to 0^+} w_1 = -\frac{1}{2}A(0). \tag{3.28}$$

By way of variation of constants, the exact solution is

$$\bar{w}_2 = -y_1(z)\int_0^z [2A(0)\bar{w}_0(s)y_2(s)]ds - y_2(z)\int_z^{+\infty} [2A(0)y_1(s)\bar{w}_0(s)]ds, \tag{3.29}$$

where y_1 and y_2 are given in Equations (3.25) and (3.26). Notice that y_1 is exponentially small and y_2 is exponentially large at infinity. It is easy to verify the matching condition by the L'Hospital's Rule.

By the asymptotic theories and the symmetry of the DSS, we composite the outer solution

and inner solution to get the asymptotic formula of the DSS in the whole domain, that is,

$$w_{comp}(x) = \begin{cases} \bar{w}_0(x/\sqrt{\epsilon}) + \epsilon\big(w_1(x) + \bar{w}_2(x/\sqrt{\epsilon}) + \frac{1}{2}A(0)\big) + \cdots, & x \geq 0, \\ -\bar{w}_0(x/\sqrt{\epsilon}) - \epsilon\big(w_1(x) + \bar{w}_2(x/\sqrt{\epsilon}) + \frac{1}{2}A(0)\big) + \cdots, & x < 0. \end{cases} \tag{3.30}$$

Here, we have already obtained the asymptotic formulas for the BGS and the DSS by asymptotic analysis. Next we go further with the study of the linear stability of the stationary solutions.

3.2 Stability/Instability

In this section, we investigate the linear stability/instability of the stationary solutions obtained in the previous section. A similar stability analysis to Section 2.2 will be applied. Thus, we assume the perturbation having the same form as Equation (2.17).

We start with the BGS, that is, we assume $v(x)$ in Equation (2.17) with the following formula

$$v(x) = w(x) = w_0 + \epsilon w_1 + \epsilon^2 w_2 + \cdots. \tag{3.31}$$

where $w(x)$ is the asymptotic formula given in (3.8). By substituting and rearranging in powers of δ, we get the linear eigenvalue problem as

$$\begin{cases} -\frac{\epsilon}{2}u_1'' + \frac{\epsilon}{2}m^2u_1 + (\epsilon A(x) - 1)u_1 + 3w^2u_1 = -\lambda u_2, \\ -\frac{\epsilon}{2}u_2'' + \frac{\epsilon}{2}m^2u_2 + (\epsilon A(x) - 1)u_2 + w^2u_2 = \lambda u_1. \end{cases} \tag{3.32}$$

Now, by Equation (3.15) we have

$$w^2 = 1 - \epsilon A(x) + \mathcal{O}(\epsilon^2).$$

Thus system (3.32) reduces to

$$\begin{cases} -\frac{\epsilon}{2}u_1'' + \frac{\epsilon}{2}m^2u_1 - 2\epsilon A(x)u_1 + 2u_1 + \mathcal{O}(\epsilon^2) = -\lambda u_2, \\ -\frac{\epsilon}{2}u_2'' + \frac{\epsilon}{2}m^2u_2 + \mathcal{O}(\epsilon^2) = \lambda u_1. \end{cases} \tag{3.33}$$

To proceed for the eigenvalue of the above system, we also consider the eigenfunctions in a specific weighted functional space. First assume the eigenfunctions satisfying $u_j(x) = f_j(x)e^{\alpha x}$, $j = 1, 2$, where α is a real number and $f_j(x) \in C^{per}[0, L]$. When substituting this formula into Equation (3.33) and writing in a matrix form, we get

$$\tilde{L}_\alpha f + \frac{\epsilon}{2}(m^2 - \alpha^2)If + \mathcal{O}(\epsilon^2) = \lambda Jf, \tag{3.34}$$

where

$$f = \begin{pmatrix} f_1 \\ f_2 \end{pmatrix}, \ \tilde{L}_\alpha = \begin{pmatrix} \tilde{L}_\alpha^+ & 0 \\ 0 & \tilde{L}_\alpha^- \end{pmatrix},$$

and

$$\begin{aligned}\tilde{L}_\alpha^+ &= -\frac{\epsilon}{2}\frac{d^2}{dx^2} - \epsilon\alpha\frac{d}{dx} - 2\epsilon A(x) + 2,\\ \tilde{L}_\alpha^- &= -\frac{\epsilon}{2}\frac{d^2}{dx^2} - \epsilon\alpha\frac{d}{dx},\end{aligned}$$

with I and J the same definition as in Equation (2.20).

To only analyze the neutral instability and the critical numbers of m for (3.34), we follow the idea in Section 2.2. By assuming $\lambda = 0$ in (3.34), we obtain

$$\begin{cases}[\tilde{L}_\alpha^+ + \frac{\epsilon}{2}(m^2 - \alpha^2)]f_1 = 0,\\ [\tilde{L}_\alpha^- + \frac{\epsilon}{2}(m^2 - \alpha^2)]f_2 = 0.\end{cases} \tag{3.35}$$

To study the above decoupled problem, we first assume

$$\begin{cases}\tilde{L}_\alpha^+\tilde{g}_1 = \tilde{k}_1\tilde{g}_1,\\ \tilde{L}_\alpha^-\tilde{g}_2 = \tilde{k}_2\tilde{g}_2,\end{cases} \tag{3.36}$$

where $\tilde{k}_1$, $\tilde{k}_2$ are the principal (smallest) eigenvalues, and $\tilde{g}_1$, $\tilde{g}_2$ are periodic functions. From the second eigenvalue problem in (3.36), we can solve it as

$$\tilde{k}_{2,n} = \epsilon\left[\frac{1}{2}\left(\frac{2n\pi}{L}\right)^2 - \alpha i\left(\frac{2n\pi}{L}\right)\right], n = 0, \pm 1, \pm 2, \cdots.$$

Thus the principal eigenvalue is $\tilde{k}_2 = \tilde{k}_{2,0} = 0$. Furthermore, $\tilde{k}_1 > \tilde{k}_2$ because of $L_\alpha^+ = L_\alpha^- + 2\,(1 - \epsilon A(x))$. By a perturbation analysis, we can obtain

$$\tilde{k}_1 = 2\left(1 - \epsilon\frac{\int_0^L A(x)dx}{L}\right).$$

Now, returning to (3.35), we will get two critical numbers m_1 and m_2. Their formulas are given as

$$m_1 = \sqrt{\alpha^2 - 2\tilde{k}_1/\epsilon} \text{ and } m_2 = |\alpha|. \tag{3.37}$$

Here, when $m = m_1$, (3.34) has a solution $\lambda = 0$ with $f_1 = \tilde{g}_1$, $f_2 = 0$; when $m = m_2$, (3.34) has a solution $\lambda = 0$ with $f_1 = 0$, $f_2 = \tilde{g}_2$. Clearly, if $\alpha^2 - 2\tilde{k}_1/\epsilon > 0$, then $m_2 > m_1 > 0$.

Next, we do the analysis on (3.35) when $m_1 < m < m_2$. Similar to Section 2.2, we can show that there exists at least one eigenvalue with $\Re(\lambda) > 0$ when $m_1 < m < m_2$.

We then consider the case where $f_j(x) \in L^2(-\infty, \infty)$ $(j = 1, 2)$. By the Floquet-Bloch theory [49], we let

$$f_j(x) = \hat{f}_j(x)e^{i\eta x},\ \hat{f}_j(x) = \hat{f}_j(x + L),\ j = 1, 2, \tag{3.38}$$

where $\eta \in [-\frac{\pi}{L}, \frac{\pi}{L}]$. Then substituting (3.38) into Equation (3.34) gives

$$\tilde{L}_{\alpha,\eta}\hat{f} + \frac{\epsilon}{2}\left[m^2 - (\alpha + i\eta)^2\right] I\hat{f} + \mathcal{O}(\epsilon^2) = \lambda J\hat{f}, \tag{3.39}$$

$$\hat{f} = \begin{pmatrix} \hat{f}_1 \\ \hat{f}_2 \end{pmatrix}, \ \tilde{L}^{\alpha,\eta} = \begin{pmatrix} L^+_{\alpha,\eta} & 0 \\ 0 & L^-_{\alpha,\eta} \end{pmatrix}, \ \beta = i\eta + \alpha,$$

and

$$\begin{aligned} \tilde{L}^+_{\alpha,\eta} &= -\frac{\epsilon}{2}\frac{d^2}{dx^2} - \epsilon(\alpha + i\eta)\frac{d}{dx} - 2\epsilon A(x) + 2, \\ \tilde{L}^-_{\alpha,\eta} &= -\frac{\epsilon}{2}\frac{d^2}{dx^2} - \epsilon(\alpha + i\eta)\frac{d}{dx}, \end{aligned}$$

where the matrices I and J have the same definitions as in (2.20). By formula (4.18) in [49] and the arguments stated in Section 2.2, we have the conclusion that when $m_1 < m < m_2$, there is at least one eigenvalue λ satisfying $\Re(\lambda) > 0$.

Lastly, we investigate the linear stability of the DSS, that is, let $v(x) = w_{comp}$ in (2.17). Thus, the eigenvalue problem is found as

$$\begin{cases} -\frac{\epsilon}{2}u_1'' + \frac{\epsilon}{2}m^2 u_1 + (\epsilon A(x) - 1)u_1 + 3w^2_{comp}u_1 = -\lambda u_2, \\ -\frac{\epsilon}{2}u_2'' + \frac{\epsilon}{2}m^2 u_2 + (\epsilon A(x) - 1)u_2 + w^2_{comp}u_2 = \lambda u_1. \end{cases} \tag{3.40}$$

Clearly, $w^2_{comp} - w^2 \to 0$ as $|x| \to \infty$. Thus, by using the theory in [16] again, we have the conclusion: the essential spectrum of the system (3.40) can be determined by the spectrum of system (3.32).

3.3 Numerical simulations

In this section, we will apply numerical simulations to validate the theoretical results from the previous section. The external potential is taken as $A(x) = V_0 \cos^2(kx)$ with $V_0 = 1$ and $k = 1$. The main difference between this case and the former one is that the chemical potential here is chosen to be relatively large; thus we do the following three steps to complete the numerical simulations.

First, we use the Newton's method to get the DSS of Equation (3.7) and then compare it with (3.30) which is obtained by the asymptotic analysis. The details are shown in Figure 3.1. The left panel shows that the numeric solution matches very well with the asymptotic solution; the right panel shows the difference between these two solutions. Thus, we have verified that the asymptotic formula is extremely accurate.

Secondly, we carry out numerical simulations to study the linear stability/instability. The computation is taken in the interval of $x \in [-2\pi, 2\pi]$. Choosing $\alpha = -5$, applying the central

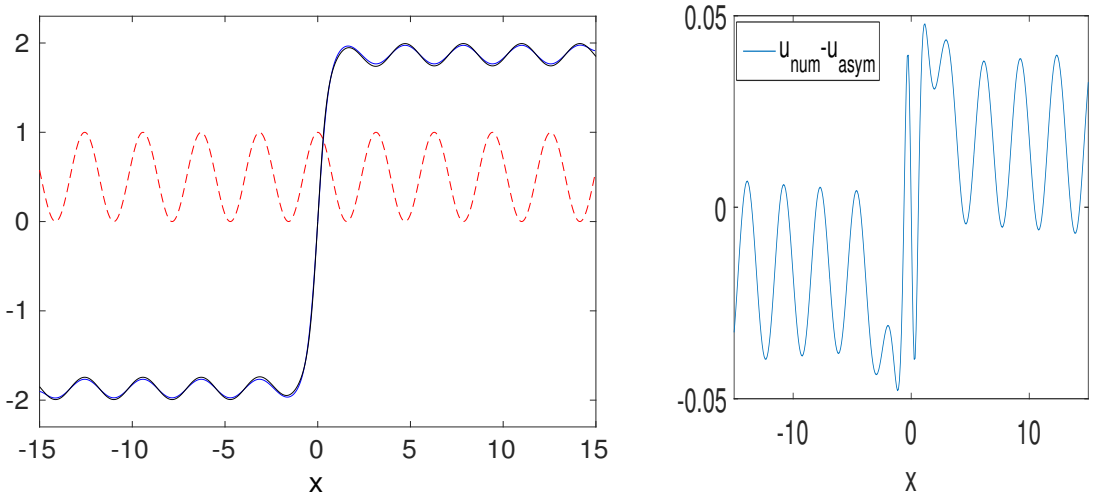

Figure 3.1: (Color online) The DSS of Equation (3.7). Parameters correspond to the parameter set: $\mu = 4$, $A(x) = \cos^2(x)$ and $x \in [-20, 20]$. In the left panel, the red dashed line is the external potential $A(x)$, the blue solid line is the solution obtained numerically and the black line is drawn based on the asymptotical formula (3.30). The right panel shows the difference between the numeric solution and the asymptotic solution.

μ	m_1	m_2
2	4.3606	5
3	3.8749	5
4	3.3192	5

Table 3.1: Critical numbers of m vs. μ. The above table is calculated in the parameter set: $\alpha = -5$ and $A(x) = \cos^2(x)$.

finite difference method and periodic boundary conditions on (3.36), and following formulas (3.37), we obtain Table 3.1. Then using the same numeric method and boundary conditions on (3.34) to get Figure 3.2. As shown in the figure, when the value of m is chosen between the corresponding critical numbers, we do have eigenvalues satisfying $\Re(\lambda) > 0$, which verifies our conclusion.

Lastly, we simulate the dynamics when the chemical potential is relatively large. The details are shown in Figures 3.3 and 3.4. To be specific, the numeric scheme used here is same as the one in Section 2.3. The simulations are performed in the domain of $(x, y) \in [-20, 20] \times [-20, 20]$; these figures show different density snapshots at indicated moments of time, where the density means the DSS's density divided by the BGS's. We have two main observations on these figures: a. the DSS will always evolve into vortices when $\mu \gg V_0$ and also oscillate horizontally when $V_0 > 0$; b. the destabilization (including evolving into vortices and oscillating along x direction) occurs earlier as the value of μ increases. These observations agree with the result shown in

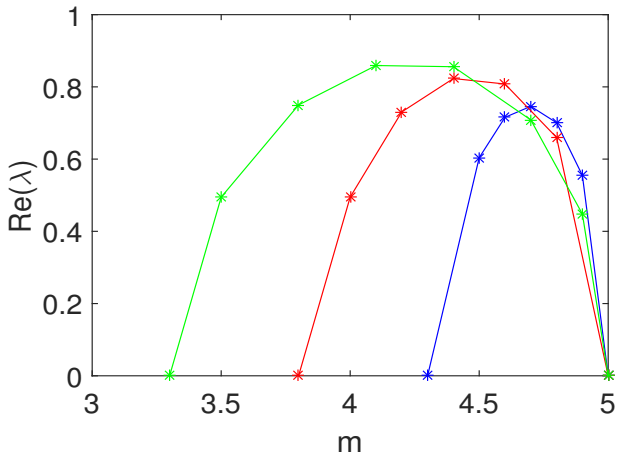

Figure 3.2: (Color online) The principal eigenvalue of (3.34) vs. m. Parameters correspond to: $\alpha = -5$ and $A(x) = \cos^2(x)$. The different curve corresponds to different value of μ. The rightmost curve (blue) corresponds to $\mu = 2$; the middle one (red) corresponds to $\mu = 3$ and the leftmost one (green) corresponds to $\mu = 4$.

Figure 3.2, i.e., the value of m_1 reduces as μ increases, which implies that the instability happens earlier.

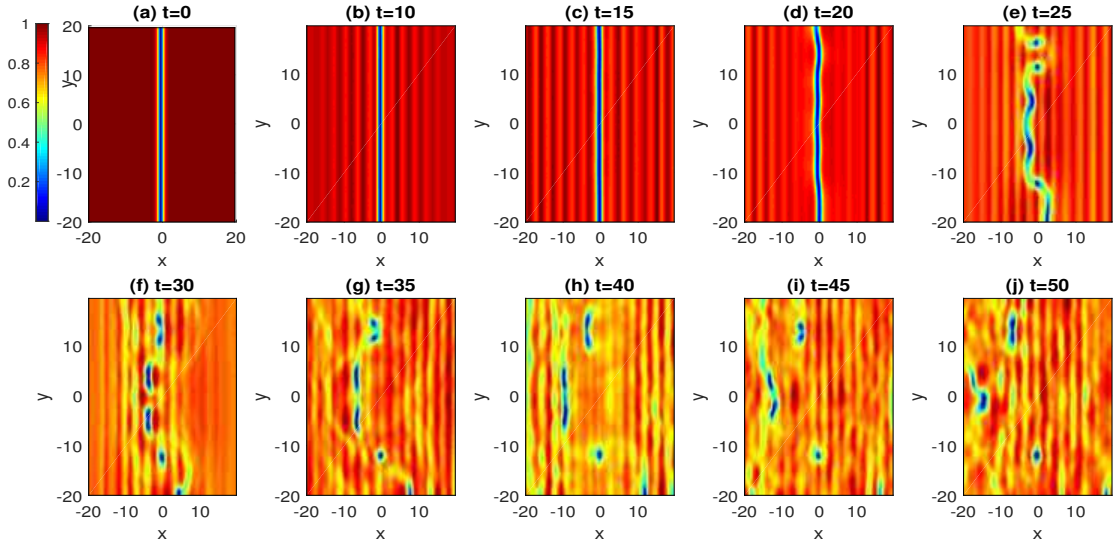

Figure 3.3: (Color online) The dynamics when $\mu = 2$.

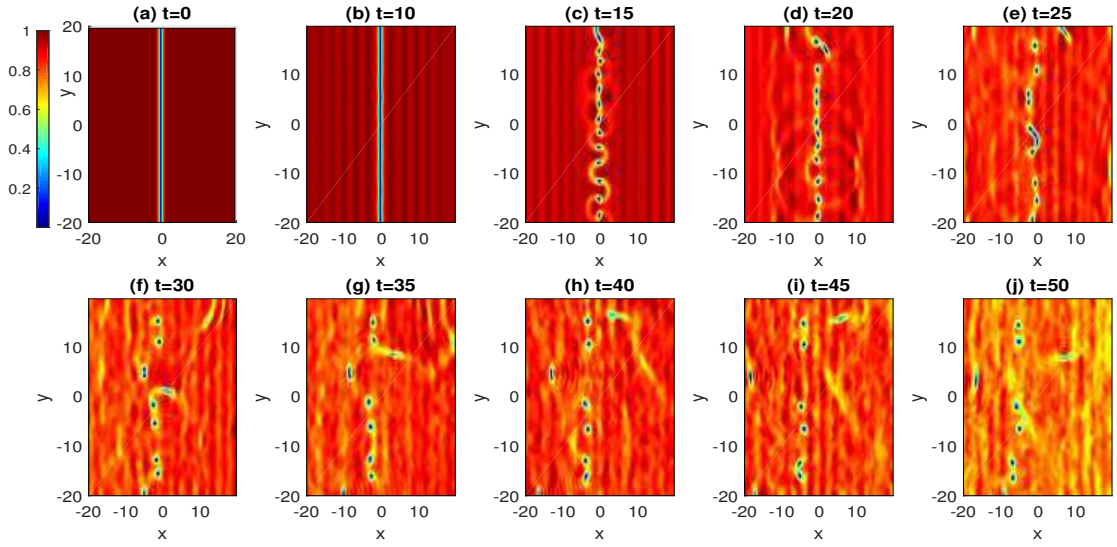

Figure 3.4: (Color online) The dynamics when $\mu = 4$.

Chapter 4

Dynamics of slowly varying external potential

In this chapter, we consider Equation (1.9) in the case where the external potential varies slowly. Thus, in Equation (1.10), we replace $A(x)$ by $A(\epsilon x)$ where A is an L-periodic function and $\epsilon \ll 1$. It is easy to see that $A(\epsilon x)$ has the period L/ϵ. For example, the function $A(\epsilon x) = \cos^2(\epsilon x)$ has a period as $\frac{\pi}{\epsilon} \gg \pi$. To be exact, we begin with the following equation

$$iv_t = -\frac{1}{2}(v_{xx} + v_{yy}) + (A(\epsilon x) - \mu)v + |v|^2 v. \tag{4.1}$$

If we let

$$z = \epsilon x,\ v(x, y, t) = v(\frac{z}{\epsilon}, y, t) = w(z, y, t), \tag{4.2}$$

then we have

$$iw_t = -\frac{1}{2}\epsilon^2 w_{zz} - \frac{1}{2}w_{yy} + (A(z) - \mu)w + |w|^2 w, \tag{4.3}$$

where $A(z)$ is a periodic function with the prime period L.

4.1 Asymptotic analysis of the stationary solutions

In this section, we proceed to use asymptotic analysis to obtain the formulas for the stationary solutions of Equation (4.3). With a proper assumption of the stationary solution being homogeneous in y direction, we seek solutions of the following equation

$$-\frac{1}{2}\epsilon^2 w_{zz} + (A(z) - \mu)w + w^3 = 0. \tag{4.4}$$

Again, due to symmetry, we have that if w is a solution, then so is $-w$. Therefore, we mainly consider the positive BGS solution in the following context. We expand the outher solution as follows

$$w = w_0 + \epsilon^2 w_2 + \cdots . \tag{4.5}$$

Substituting (4.5) into (4.4), we obtain the following equations at different orders.

Up to $\mathcal{O}(\epsilon^0)$, we get

$$\begin{cases} (A(z)-\mu)w_0 + w_0^3 = 0, \\ w_0(z) = w_0(z+L). \end{cases} \tag{4.6}$$

Solving the above system gives

$$w_0(z) = \sqrt{\mu - A(z)}. \tag{4.7}$$

Up to $\mathcal{O}(\epsilon^2)$, we obtain

$$\begin{cases} -\frac{1}{2}w_0'' + (A(z)-\mu)w_2 + 3w_0^2 w_2 = 0, \\ w_2(z) = w_2(z+L). \end{cases} \tag{4.8}$$

Solving for w_2, we have

$$w_2(z) = \frac{(\sqrt{\mu - A(z)})''}{4(\mu - A(z))}. \tag{4.9}$$

Thus, we arrive at the positive BGS's asymptotic formula

$$w = \sqrt{\mu - A(z)} + \epsilon^2 \frac{(\sqrt{\mu - A(z)})''}{4(\mu - A(z))} + \cdots . \tag{4.10}$$

As for the DSS, we again use boundary theory to find the approximate formula. Undoubtedly, there is a boundary layer near $x = 0$. Away from this point, by symmetry, its outer approximation is given by

$$w = \begin{cases} w_0 + \epsilon^2 w_2 + \cdots , \ z > 0, \\ -w_0 - \epsilon^2 w_2 + \cdots , \ z < 0. \end{cases} \tag{4.11}$$

Here, w_0 and w_2 are shown in (4.7) and (4.9).

For the inner solution (near $x = 0$), we need the following transformation

$$\xi = \frac{z}{\epsilon}, \ w(z) = w(\epsilon\xi) = W(\xi), \ A(z) = A(\epsilon\xi). \tag{4.12}$$

Thus

$$w' = \frac{1}{\epsilon}W', \ w'' = \frac{1}{\epsilon^2}W''. \tag{4.13}$$

Equation (4.4) becomes

$$-\frac{1}{2}W'' + (A(\epsilon\xi) - \mu)W + W^3 = 0. \tag{4.14}$$

We expand the external potential $A(\epsilon\xi)$ as

$$A(\epsilon\xi) = A(0) + \epsilon A'(0)\xi + \frac{\epsilon^2}{2}A''(0)\xi^2 + \cdots , \tag{4.15}$$

and assume W as

$$W = W_0 + \epsilon W_1 + \epsilon^2 W_2 + \cdots . \tag{4.16}$$

Substituting all of them into Equation (4.14) gives equations for W_0 and W_1.

For W_0, we have

$$\begin{cases} -\frac{1}{2}W_0'' + (A(0) - \mu)W_0 + W_0^3 = 0, \\ W_0(0) = 0 \end{cases} \tag{4.17}$$

subject to a matching condition

$$\lim_{\xi \to +\infty} W_0(\xi) = \lim_{x \to 0^+} w_0 = \sqrt{\mu - A(0)}. \tag{4.18}$$

Solving the above system gives

$$W_0(\xi) = \sqrt{\mu - A(0)} \tanh(\sqrt{\mu - A(0)}\xi),\ \xi \geq 0. \tag{4.19}$$

For W_1, we obtain

$$\begin{cases} -\frac{1}{2}W_1'' - (\mu - A(0))W_1 + 3W_0^2 W_1 + A'(0)\xi W_0 = 0, \\ W_1(0) = 0. \end{cases} \tag{4.20}$$

The corresponding matching condition is

$$W_1(\infty) = 0. \tag{4.21}$$

In particular, if $A'(0) = 0$, it is easy to get $W_1 = 0$.

Taking the asymptotic theories and the symmetry of the DSS into account and combining the outer solution with the inner solution, we get the DSS as

$$v(z) = \begin{cases} w_0(z) + W_0(z/\epsilon) - \sqrt{\mu - A(0)} + \cdots ,\ z \geq 0, \\ -w_0(z) - W_0(z/\epsilon) + \sqrt{\mu - A(0)} + \cdots ,\ z < 0. \end{cases} \tag{4.22}$$

Here, w_0 and W_0 are given in Equations (4.7) and (4.19). Now, with the obtained formulas for the BGS and the DSS by asymptotic analysis, we are ready to study the linear stability/instability of these stationary solutions.

4.2 Stability/Instability

In this section, we will study the linear stability/instability of these stationary solutions when the external potential varies slowly. The method used here is similar to the one used in Section 2.2 (or Section 3.2). Thus, we also assume the perturbation with the same form as Equation (2.17).

We start with the investigation on the linear stability of the BGS; so in Equation (2.17) we let $U(z) = w(z)$ with $w(z)$ defined in (4.10). Then, by substituting this formula into Equation (4.3) and considering the linear independence of $e^{\lambda t}e^{imy}$ and $e^{\lambda^\star t}e^{-imy}$, we get the linear eigenvalue problem as follows

$$\begin{cases} -\frac{1}{2}\epsilon^2 u_1'' + \frac{1}{2}m^2 u_1 + (A(z)-\mu)u_1 + 3w^2 u_1 = -\lambda u_2, \\ -\frac{1}{2}\epsilon^2 u_2'' + \frac{1}{2}m^2 u_2 + (A(z)-\mu)u_2 + w^2 u_2 = \lambda u_1. \end{cases} \tag{4.23}$$

In view of

$$w^2 = \mu - A(z) + 2\epsilon^2 w_0 w_2 + \mathcal{O}(\epsilon^4),$$

the above system (4.23) can be simplified as

$$\begin{cases} -\frac{1}{2}\epsilon^2 u_1'' + \frac{1}{2}m^2 u_1 + 2(\mu - A(z))u_1 + 6\epsilon^2 w_0 w_2 u_1 + \mathcal{O}(\epsilon^4)u_1 = -\lambda u_2, \\ -\frac{1}{2}\epsilon^2 u_2'' + \frac{1}{2}m^2 u_2 + 2\epsilon^2 w_0 w_2 u_2 + \mathcal{O}(\epsilon^4)u_2 = \lambda u_1. \end{cases} \tag{4.24}$$

Similar to Section 2.2, we introduce the weighted function space. That is, we seek the solution with the following form $u_j(x) = f_j(x)e^{\alpha x}$, $j = 1, 2$, where α is a real number. We first assume that $f_j(x) \in \mathcal{C}^{per}[0, L]$. After substituting this formula into Equation (4.24) and writing in a matrix form, we have

$$\hat{L}f + \frac{1}{2}(m^2 - \epsilon^2\alpha^2)If + \mathcal{O}(\epsilon^4) = \lambda Jf. \tag{4.25}$$

$$f = \begin{pmatrix} f_1 \\ f_2 \end{pmatrix}, \ \hat{L} = \begin{pmatrix} \hat{L}_+ & 0 \\ 0 & \hat{L}_- \end{pmatrix},$$

and

$$\begin{aligned} \hat{L}_+ &= -\epsilon^2 \frac{1}{2}\frac{d^2}{dz^2} - \epsilon^2\alpha\frac{d}{dz} + 2(\mu - A(z)) + 6\epsilon^2 w_0 w_2, \\ \hat{L}_- &= -\epsilon^2 \frac{1}{2}\frac{d^2}{dz^2} - \epsilon^2\alpha\frac{d}{dz} + 2\epsilon^2 w_0 w_2, \end{aligned}$$

where I and J are defined in (2.20).

Again, we first want to do analysis on the neutral instability and find the critical numbers of m for (4.25). Following Section 2.2, by assuming $\lambda = 0$ in (4.25), we get

$$\begin{cases} \left[\hat{L}_+ + \frac{1}{2}(m^2 - \epsilon^2\alpha^2)\right] f_1 = 0, \\ \left[\hat{L}_- + \frac{1}{2}(m^2 - \epsilon^2\alpha^2)\right] f_2 = 0, \end{cases} \tag{4.26}$$

To investigate the above decoupled problem, we first consider

$$\begin{cases} \hat{L}_+ \hat{g}_1 = \hat{k}_1 \hat{g}_1, \\ \hat{L}_- \hat{g}_2 = \hat{k}_2 \hat{g}_2, \end{cases} \tag{4.27}$$

where $\hat{k}_j$ is the principal (smallest) eigenvalues, and $\hat{g}_j(x) = \hat{g}_j(x+L) \not\equiv 0,\ j = 1, 2$. By comparison, we have $k_1 > k_2$, since $\hat{L}_+ = \hat{L}_- + 2w^2$. When returning to (4.26), we get two critical numbers m_1 and m_2 with the formulas

$$m_1 = \sqrt{\epsilon^2\alpha^2 - 2k_1} \ \text{ and } \ m_2 = \sqrt{\epsilon^2\alpha^2 - 2k_2}. \tag{4.28}$$

The above statements lead to the conclusion: when $m = m_1$, (4.25) has a solution $\lambda = 0$ with $f_1 = \hat{g}_1$ and $f_2 = 0$; when $m = m_2$, (4.25) has another solution $\lambda = 0$ with $f_1 = 0$ and $f_2 = \hat{g}_2$. Moreover, if $\epsilon^2\alpha^2 - 2k_1 > 0$, then $m_2 > m_1 > 0$.

Through similar arguments discussed in Section 2.2, we can also have that (4.25) has at least one eigenvalue with $\Re(\lambda) > 0$ when $m_1 < m < m_2$.

Next, we consider the case when $f_j(x) \in \mathcal{L}(-\infty, \infty)$ $(j = 1, 2)$. Again, we apply the Floquet-Bloch theory [49] and let

$$f_j(x) = \hat{f}_j(x) e^{i\eta x},\ \hat{f}_j(x) = \hat{f}_j(x+L),\ j = 1, 2, \tag{4.29}$$

where $\eta \in [-\frac{\pi}{L}, \frac{\pi}{L}]$. Substituting Equation (4.29) into Equation (4.25) gives

$$\hat{L}^\beta \hat{f} + \frac{1}{2}(m^2 - \epsilon^2\beta^2) I \hat{f} + \mathcal{O}(\epsilon^4) = \lambda J \hat{f}, \tag{4.30}$$

where

$$\hat{f} = \begin{pmatrix} \hat{f}_1 \\ \hat{f}_2 \end{pmatrix},\ \hat{L}^\beta = \begin{pmatrix} \hat{L}_+^\beta & 0 \\ 0 & \hat{L}_-^\beta \end{pmatrix},\ \beta = i\eta + \alpha,$$

and

$$\begin{aligned} \hat{L}_+^\beta &= -\epsilon^2 \frac{1}{2}\frac{d^2}{dx^2} - \epsilon^2\beta\frac{d}{dx} + 2(\mu - A(z)) + 6\epsilon^2 w_0 w_2, \\ \hat{L}_-^\beta &= -\epsilon^2 \frac{1}{2}\frac{d^2}{dx^2} - \epsilon^2\beta\frac{d}{dx} + 2\epsilon^2 w_0 w_2, \end{aligned}$$

where I, J defined in (2.20). Similarly, we claim that there is at least one eigenvalue satisfying $\Re(\lambda) > 0$ when m is between m_1 and m_2.

To investigate the linear stability of the DSS, we let $U(x) = v(x)$ in Equation (2.17), where $v(x)$ is defined in Equation (4.22). The corresponding linear eigenvalue problem can be found as

$$\begin{cases} -\frac{1}{2}\epsilon^2 u_1'' + \frac{1}{2}m^2 u_1 + (A(z) - \mu)u_1 + 3v^2 u_1 = -\lambda u_2, \\ -\frac{1}{2}\epsilon^2 u_2'' + \frac{1}{2}m^2 u_2 + (A(z) - \mu)u_2 + v^2 u_2 = \lambda u_1. \end{cases} \tag{4.31}$$

Notice that $v^2 - w^2 \to 0$ as $x \to \infty$. Thus, by [16], we have claim that the essential spectrum points of the system (4.31) can be derived from the spectrum of system (4.23).

4.3 Numerical simulations

In this section, we will carry out numerical simulations when the external potential is almost a constant. We take $A(x) = V_0 \cos^2(\epsilon x)$ with $V_0 = 1$. The chemical potential is fixed as $\mu = 1.05$.

First, we want to verify the asymptotic formula of the DSS (4.22). To proceed, we apply the Newton's method on (4.4) to get the numeric DSS and then compare it with the formula (4.22). The details are shown in Figure 4.1. The left panel shows that the asymptotic solution matches well with the numeric one; the right panel reveals the difference between these two solutions. Thus, we conclude that the solution formula (4.22) is accurate.

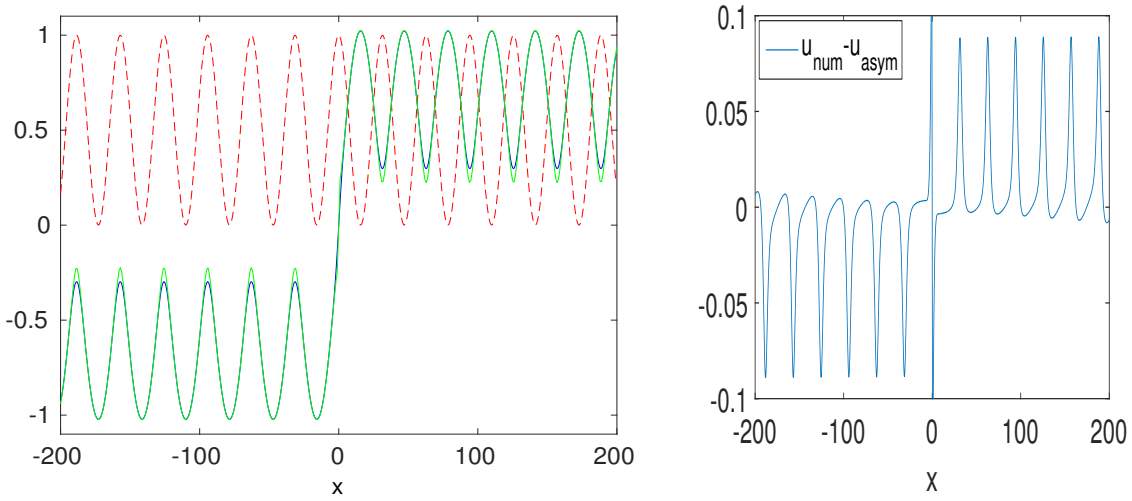

Figure 4.1: (Color online) The DSS in the case of slowly varying external potential. The figures correspond to the parameter set: $\mu = 1.05$, $A(x) = \cos^2(0.1x)$ and $x \in [-200, 200]$. In the left panel, the dashed red line denotes the external potential, the blue thin line directly comes from the numerical simulation and the light green thin line is the asymptotic formula (4.22). The right panel gives the difference between the numeric solution and the asymptotic formula.

Secondly, we numerically compute the critical wave numbers corresponding to different values of ϵ. To have m_1 being meaningful, we choose α large enough as $\alpha = -30$. By applying the central difference method with periodic boundary conditions on (4.27) and based on the formulas (4.28), we get Table 4.1. As shown in the table, when the value of ϵ decreases slightly, the value of m_1 (m_2) reduces a lot. Then, based on Table 4.1, we use the same numeric scheme and boundary conditions on (4.25) and depict Figure 4.2, which reveals the relationship between the real part of eigenvalue λ and the frequency m. As we can see in this figure, if we choose m between the two critical wave numbers, the real part of the principal eigenvalue of (4.25) will be positive, i.e., $\Re(\lambda) > 0$.

ϵ	m_1	m_2
0.05	1.2724	1.4988
0.08	1.9915	2.3982
0.10	2.6092	2.9977

Table 4.1: Critical numbers of m vs. ϵ. The table is calculated in the interval $x \in [-200, 200]$.

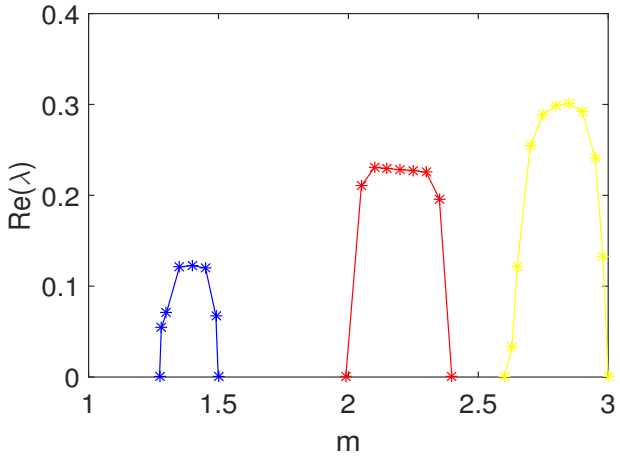

Figure 4.2: (Color online) The principal eigenvalue of the (4.25) vs. m. The figure corresponds to the parameter set: $\mu = 1.05$, $\alpha = -30$, $A(x) = \cos^2(\epsilon x)$ and $x \in [-200, 200]$. The leftmost curve (blue) denotes the case where $\epsilon = 0.05$, the middle one (red) is $\epsilon = 0.08$ and the rightmost one (yellow) corresponds to $\epsilon = 0.1$.

Lastly, we capture the dynamics of transverse modulation instability. The same numeric scheme with Neumann boundary conditions as Section 2.3 is used here. The details are shown in Figures 4.3 and 4.4. The simulations are carried out in the domain of $(x, y) \in [-20, 20] \times [-20, 20]$; these figures show different density snapshots at indicated moments of time, where the density is the DSS's density divided by the BGS's. As shown in these figures, the DSS starts to move to the right when $t = 105$ and $\epsilon = 0.1$; the DSS starts to move to the left when $t = 190$ and $\epsilon = 0.05$. This phenomenon indicates, when $V_0 \sim \mu$, the DSS only oscillates horizontally and keep still longer as the value of ϵ decreases. These observations match the results from Figure 4.2, i.e., when the value of $\Re(\lambda)$ reduces as ϵ decreases, which implies that instability becomes weaker.

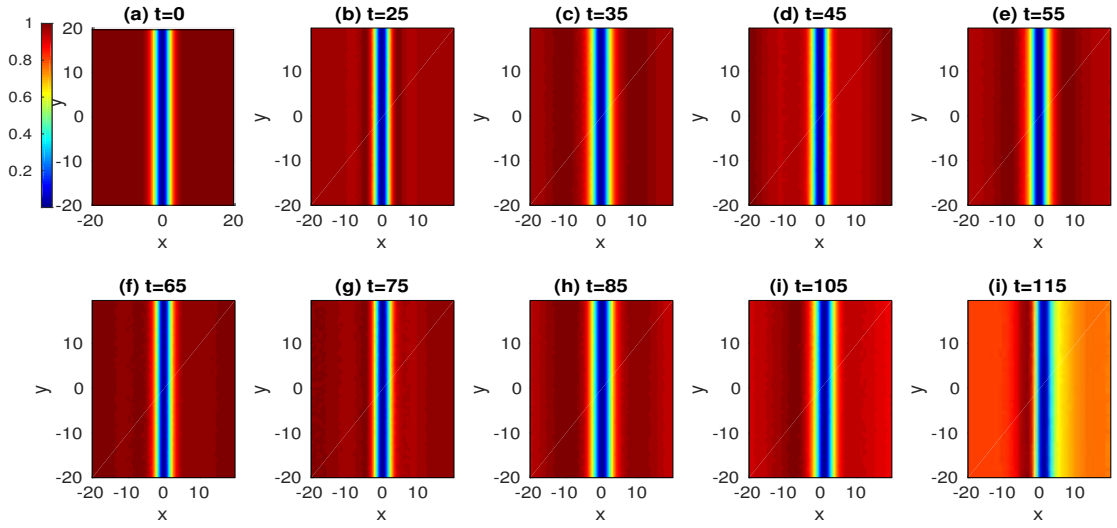

Figure 4.3: (Color online) The dynamics when $\epsilon = 0.1$.

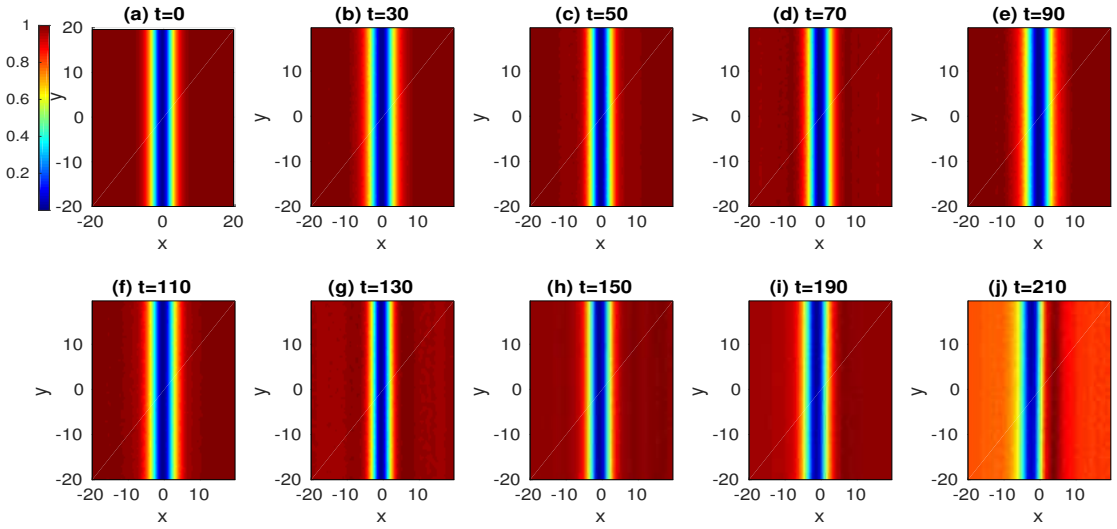

Figure 4.4: (Color online) The dynamics when $\epsilon = 0.05$.

Chapter 5

Summary and future work

In this thesis, we have studied the existence and linear stability/instability of the BGS and the DSS of Equation (1.10). We have proved the existence of the BGS by dynamical systems theory and investigated the asymptotic behavior of the DSS as $x \to \pm\infty$. Then we analytically found the critical wave numbers of m when $\lambda = 0$ in Equation (2.23) by extending the method in [31]. A constant potential was applied to illustrate our analysis. To give a visual view, we have applied some numeric methods to depict the stationary solutions, find the exact critical wave numbers, and capture the transverse modulational instabilities for some specifically chosen parameter sets.

In the case of large chemical potential, i.e. $\mu \gg 1$, we have obtained the solution formulas of the BGS and the DSS by means of asymptotic approximation. In term of those formulas, we have analyzed the linear stability for the BGS and DSS. Actually, we have found that the minimal critical wave number depends closely on the value of the chemical potential as shown in Equation (3.37). By numerical simulations, we have verified that the asymptotic formula (3.30) is extremely accurate and also found that the minimal critical wave number decreases when the chemical potential increases.

In the case of slowly varying external potential, i.e., $A = A(\epsilon x)$ ($\epsilon \ll 1$), we also have obtained the solution formulas of the BGS and the DSS by the asymptotic method. Based on the asymptotic solution formulas, we have derived the formulas for the critical wave numbers as shown in Equation (4.28). Then, under some appropriate choices on ϵ and with the direct numerical computations, we have confirmed the accuracy of the formulas obtained by the asymptotic analysis. The exact values of the corresponding critical wave numbers also have been calculated.

The results presented here are straightforward, feasible and can be easily confirmed by numerical simulations, and the method used can be naturally extended to other external potentials. It would be interesting to investigate the stability properties of 2D solitons with self-attraction in the model with an attractive force. Another interesting challenging problem is to study the stability of the traveling wave solutions when external potentials moving with a speed, for example, $A(x) \to A(x - vt)$ for some $v \in \mathbb{R}$.

Bibliography

[1] M. J. Ablowitz and H. Segur, "Solitons and the inverse scattering tranform", Society for Industrial and Applied Mathematics (SIAM), Philadelphia, 1981.

[2] G. L. Alfimov, V. V. Konotop and M. Salerno, *Matter solitons in Bose-Einstein condensates with optical lattices*, Europhys. Lett., **58** (2002), 7–13.

[3] D. Anderson, *Variational approach to nonlinear pulse propagation in optical fibers*, Phys. Rev. A, **27** (1983), 3135–3145.

[4] I. V. Barashenkov, *Stability criterion for dark solitons*, Phys. Rev. Lett., **77** (1996), 1193-1196.

[5] N. Bogolobov, *On the thory of superfluidity*, J. Phys., **11** (1947), 23–32.

[6] A. D. Bouard, *Instability of stationary bubble*, SIAM J. Math. Anal., **26** (1995), 566–582.

[7] V. A. Brazhnyi and V. V. Konotop, *Theory of nonlinear matter waves in optical lattices*, Mod. Phys. Lett. B, **18** (2004), 627.

[8] L. D. Carr, C. W. Chark and W. P. Reinhardt, *Stationary solutions of the one-dimensional nonlinear Schrödinger equation: I. case of repulsive nonlinearity*, Phys. Rev. A, **62** (2000), 063610.

[9] L. D. Carr, C. W. Chark and W. P. Reinhardt, *Stationary solutions of the one-dimensional nonlinear Schrödinger equation: II. case of attractive nonlinearity*, Phys. Rev. A, **62** (2000), 063611.

[10] R. Carretero-Gonzaález, D. J. Frantzeskakis and P. G. Kevrekidis, *Nonlinear waves in Bose-Einstein condensates: physical relevance and mathematical techniques*, Nonlinearity, **21** (2008), R139–R202.

[11] F. Dalfovo, S. Giorgini, L. P. Pitaevskii and S. Stringari, *Theory of Bose-Einstein condensation in trapped gases*, Rev. Mod. Phys., **71** (1999), 463–531.

[12] L. Debnath, "Nonlinear partial differntial equations for scientists and engineers (third edition)", Springer Science+Business Media, New York, 2012.

[13] P. G. Dranzin and R. S. Johnson, "Solintons: an introduction", Cambridge University Press, Cambridge, 1996.

[14] D. J. Frantzeskakis, *Dark solitons in atomic Bose-Einstein condensates: from theory to experiments*, J. Phys. A: Math. Theor., **43** (2010), 213001.

[15] E. P. Gross, *Hydrodynamics of a superfluid condensate*, J. Math. Phys., **4** (1963), 195–207.

[16] D. Henry, "Geometric theory of semilinear parabolic equations", Lect. Notes in Math. Vol. 840, Springer-Verlag, Berlin Heideberg New York, 1981.

[17] E. Kengne and R. Vaillancourt, *Exact solutions of the Gross-Pitaevskii equation in periodic potential in the presence of external source*, J. Math. Phys., **48** (2007), 073520.

[18] P. G. Kevrekidis, R. Carretero-González, G. Theocharis, D. J. Frantzeskakis and B. A. Malomed, *Stability of dark solitons in Bose-Einstein condensate trapped in an optical lattice*, Phys. Rev. A, **68** (2003), 035602.

[19] P. G. Kevrekidis, D. J. Frantzeskakis and R. Carretero-González, "Emergent nonlinear phenomena in Bose-Einstein condensates: theory and experiment", Springer-Verlag, Berlin Heidelberg, 2008.

[20] Y. S. Kivshar and B. Luther-Davies, *Dark optical solitons: physics and applications*, Phys. Rept. **298** (1998), 81-197.

[21] Y. S. Kivshar and W. Krolikowski, *Lagrangian approach for dark solitons*, Opt. Comun., **114** (1995), 353–362.

[22] Y. S. Kivshar, J. Chrsto, V. Tikhonenko, B. Luther-Davies and L. M. Pismen, *Dynamics of optical vortex solitons*, Opt. Commun., **152** (1998), 198–206.

[23] V. V. Konotop and M. Salerno, *Modulational instability in Bose-Einstein condensates in optical lattices*, Phys. Rev. A, **65** (2002), 021602.

[24] V. V. Konotop and V. E. Vekslerchik, *Direct perturbation theory for dark solitons*, Phys. Rev. E., **49** (1994), 2397–2407.

[25] E. A. Kuznetsov and S. K. Turistsyn, *Instability and collapse of solitons in media with a defocusing nonlinearity*, Zh. Eksp. Teor. Fiz., **94** (1988), 119-129 [Sov. Phys. JETP, **67** (1988), 1583-1588].

[26] E. H. Lieb, R. Seiringer and J. Yngvason, *Bosons in a trap: a rigorous derivation of the Gross-Pitaevskii energy functional*, Phys. Rev. A, **61** (2000), 759–771.

[27] Z. Lin, *Stationary and instability of traveling solitonic bubbles*, Adv. Diff. Eqs., **7** (2002), 897–918.

[28] P. J. Louis, E. A. Ostrovskaya and Y. S. Kivshar, *Matter-wave dark solitons in optical lattices*, J. Opt. B, **6** (2004), S309–S317.

[29] M. Ma and Z. Huang, *Bright soliton solution of a Gross-Pitaevskii equation*, App. Math. Lett., **26** (2013), 718–724.

[30] M. Ma, C. Dang and Z. Huang, *Analytical expressions for dark solitons solution for a Gross-Pitaevskii equation*, App. Math. Comp., **273** (2016), 383–389.

[31] M. Ma, R. Carretero-González, P. G. Kevrekidis, D. J. Frantzeskakis and B. A. Malomed, *Controlling the transverse instability of dark solitons and nucleation of vortices by a potential barrier*, Phys. Rev. A, **82** (2010), 023621.

[32] M. Maris, *Stationary solutions to a nonlinear Schrödinger equation with potential in one dimension*, Proc. Roy. Soc. Edingburgh A, **133** (2003), 409–437.

[33] J. T. MendonÇa and H. TerÇas, "Physics of ultra-cold matter: atomic clouds, Bose-Einstein condensates and Rydberg plasmas", Springer Science+Business Media, New York, 2012.

[34] L. D. Menza and C. Gallo, *The black solitons of one-dimensional NLS equation*, Nonlinearity, **20** (2007), 461–496.

[35] Z. G. Ouyang and C. H. Ou,*Gloabal stability and convergence rate of traveling waves for a nonlocal model in periodic media*, DCDS-B, **17** (2015), 993-107.

[36] N. G. Parker, N. P. Proukakis, C. F. Barenchi and C. S. Adams, *Dynamical instability of a dark soliton in a quasi-one-dimensional Bose-Einstein condensate perturbed by an optical lattice*, J. Phys. B, **37** (2004), S175–S185.

[37] D. E. Pelinovsky, A. A. Sukhorukov and Y. S. Kivshar, *Bifurcation and stability of gap solitons in periodic potentials*, Phys. Rev. E, **70** (2004), 036618.

[38] D. E. Pelinovsky and P. G. Kevrekidis, *Dark solitons in external potentials*, Z. angew. Math. Phys., **59** (2008), 559–699.

[39] D. E. Pelinovsky, D. J. Frantzeskakis and P. G. Kevrekidis, *Oscillations of dark solitons in the trapped Bose-Einstein condensates*, Phys. Rev. E, **72** (2005), 016615.

[40] D. E. Pelinovsky, Y. S. Kivshar and V. V. Afanasjev, *Instability-induced dynamicas of dark soliton*, Phys. Rev. E, **54** (1996), 2015–2032.

[41] L. P. Pitaevskii and S. Stringari, "Bose-Einsten Condensation", Clarendon Press, Oxiford, 2003.

[42] L. P. Pitaevskii, *Vortex lines in an imperfect Bose gas*, Zh. Eksp. Teor. Fiz., **40** (1961), 646–651 [Sov. Phys. JETP. **13** (1961), 451–454].

[43] J. S. Russell, *Report on waves*, Fourteenth meeting of the BA., York, (1844), 311–390 [London, 1845].

[44] B. Sandstede and A. Scheel, *Absolute and convective instabilities of waves on unbounded and large bounded domains*, Phys. D, **145** (2000), 233–277.

[45] A. C. Scott, F. Y. Chu and D. W. Mclaughlin, *The soliton: a new concept in applied science*, Proceedings of IEEE, **61** (1973), 1443-1483.

[46] G. Theocharis, D. J. Frantzeskakis, R. Carretero-González, P. G. Kevrekidis and B. A. Malomed, *Controlling the motion of dark solitons by means of periodic potentials: application to Bose-Einstein condensates in optical lattices*, Phys. Rev. E, **71** (2005), 017602.

[47] G. Theocharis, P. Schmelcher, P. G. Kevrekidis and D. J. Frantzeskakis, *Matter-wave solitons of collisionally inhomogeneous condensates*, Phys. Rev. A, **72** (2005), 033614.

[48] P. J. Torrs and V. V. Konotop, *On the existence of dark solitons in a cubic-quintic nonlinear Schrödinger equation with a periodic potential*, Commun. Math. Phys., **282** (2008), 1–9.

[49] D. Tseluiko, M. G. Blyth and D. T. Papageorgiou, *Stability of film flow over inclined topography based on a long-wave nonlinear model*, J. Fluid Mech., **729** (2013), 638–671.

[50] T. Tsuzuki, *Nonlinear waves in the Pitaevskii-Gross equation*, J. Low Temp. Phys., **4** (1971), 441–457.

[51] I. M. Uzunov and V. S. Gerdjikov, *Self-frequency shift of dark solitons in optical fibers*, Phys. Rev. A, **47** (1993), 1582-1585.

[52] A. Wazwaz, "Partial differential equations and solitary waves theory", Higer educations press and Springer-Verlag Berlin Heidelberg, 2009.

[53] Z. Y. Yan and F. C. Yan, *Dark solitons for the defocusing cubic nonlinear Schrödinger equation with spatially periodic potential and nonlinearity*, Commun. Theor. Phys., **64** (2015), 309–319.

[54] N. J. Zabusky and M. D. Kruskal, *Interaction of "Solitons" in a collisionless plasma and the recurrence of initial states*, Phys. Rev. Lett., **15** (1965), 240–243.

[55] V. E. Zakharov and A. B. Shabat, *Exact theory of two-dimensional self-focusing and one dimensional self-modulation of waves in nonlinear media*, Zh. Eksp. Teor. Fiz., **61** (1971), 118-134 [Sov. Phys. JETP, **34** (1972), 62–69].

[56] V. E. Zakharov and A. B. Shabat, *Interaction between solitons in a stable medium*, Zh. Eksp. Teor. Fiz., **64** (1973), 1627-1639 [Sov. Phys. JETP, **37** (1973), 823–835].

[57] X. Q. Zhao, "Dynamical systems in population biology", Springer-Verlag, New York, 2003.

Appendix A

A constant case

To illustrate the analysis of the eigenvalue problem in the Section 2.2, we consider a constant case. Let $A(x) \equiv A$ for some constant $A < \mu$. We have the BGS solution $U(x) = \sqrt{\mu - A}$. Set $B = U(x)^2 = \mu - A$. Clearly, constants are still periodic functions which satisfy our boundary conditions. Thus the eigenvalue problem (2.23) reduces to

$$\begin{cases} -\frac{1}{2}f_1'' - \alpha f_1' + c_1 f_1 = -\lambda f_2, \\ -\frac{1}{2}f_2'' - \alpha f_2' + c_2 f_2 = \lambda f_1, \end{cases} \tag{A.1}$$

where $c_1 = 2\mu - 2A + \frac{1}{2}(m^2 - \alpha^2)$ and $c_2 = \frac{1}{2}(m^2 - \alpha^2) = c_1 - 2B$. Combining those two equations gives a fourth order differential equation as follows

$$\frac{1}{4}\frac{d^4 f_2}{dx^4} + \alpha\frac{d^3 f_2}{dx^3} + \left(-\frac{c_1 + c_2}{2} + \alpha^2\right)\frac{d^2 f_2}{dx^2} - \alpha(c_1 + c_2)\frac{df_2}{dx} + c_1 c_2 f_2 = -\lambda^2 f_2. \tag{A.2}$$

Since $f_2(x)$ is an L-periodic function, we let $f_2(x) = e^{i\tau x}$ and $\tau = \frac{2n\pi}{L}$, where $n = 0, \pm 1, \pm 2, \cdots$ and i denotes the imaginary unit. After substituting $e^{i\tau x}$ into Equation (A.2), we get

$$\frac{1}{4}\tau^4 - \alpha\tau^3 i + \left(-\frac{c_1 + c_2}{2} + \alpha^2\right)(-\tau^2) - \alpha(c_1 + c_2)\tau i + c_1 c_2 = -\lambda^2. \tag{A.3}$$

Separating the real and imaginary part, we obtain

$$\begin{cases} \Re(\lambda^2) = \frac{1}{4}\tau^4 - \left(-\frac{c_1+c_2}{2} + \alpha^2\right)\tau^2 + c_1 c_2, \\ \Im(\lambda^2) = -\alpha\tau^3 - \alpha(c_1 + c_2)\tau. \end{cases} \tag{A.4}$$

Specifically, we let $\lambda = a + bi$, $a, b \in \mathbb{R}$, then $\lambda^2 = a^2 - b^2 + 2abi$; thus

$$\begin{cases} -(a^2 - b^2) = \frac{1}{4}\tau^4 - \left(-\frac{c_1+c_2}{2} + \alpha^2\right)\tau^2 + c_1 c_2, \\ -2ab = -\alpha\tau^3 - \alpha(c_1 + c_2)\tau. \end{cases} \tag{A.5}$$

Solving the above system for a, b, we get the expressions for a and b as

$$\begin{cases} b_{\pm} = \pm\sqrt{\frac{S_1 \pm \sqrt{S_1^2+S_2^2}}{2}}, \\ a_{\pm} = \frac{S_2}{2b_{\pm}}, \end{cases} \tag{A.6}$$

where

$$\begin{cases} S_1 = \frac{1}{4}\tau^4 - (-\frac{c_1+c_2}{2} + \alpha^2)\tau^2 + c_1c_2, \\ S_2 = \alpha\tau^3 + \alpha(c_1+c_2)\tau. \end{cases} \tag{A.7}$$

Based on the above expressions, we have the result that the real part $a(\tau)$ is an odd function of τ and the imaginary part $b(\tau)$ is an even function in τ. It is clear to see that if λ is an eigenvalue of (A.2), so are also $-\lambda$, λ^* and $-\lambda^*$. Thus, in Figure A.1, we illustrate the curves by only choosing the "plus" parts of a and b.

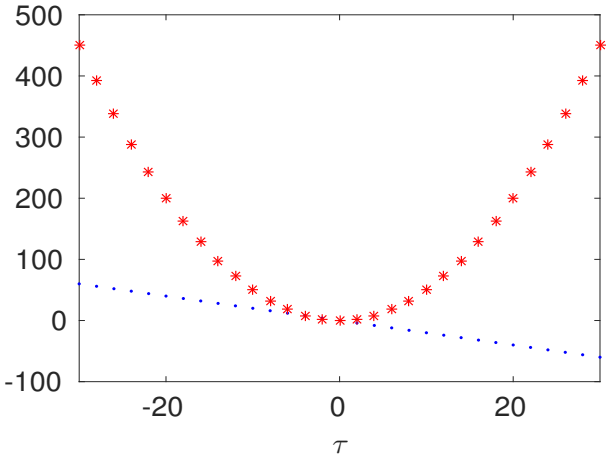

Figure A.1: (Color online) The eigenvalues of the fourth order problem (A.2). Parameters correspond to the parameter set: $\mu = 1$, $m = 2$, $\alpha = -2$, $A(x) = 0$, $U(x) = 1$ and $n = -15, -14, ..., 14, 15$; thus $c_1 = 2$ and $c_2 = 0$. The red stars denote b_+, and the blue dots represent a_+.